(52)

JPO, 1999

Ocean Turbulence I: one–point closure model

Momentum and heat vertical diffusivities

V.M. Canuto[1,2], A. Howard[1], Y. Cheng[1] and M. S. Dubovikov[1]

[1]NASA Goddard Institute for Space Studies

2880 Broadway, N.Y., N.Y., 10025

[2]Dept. Applied Physics, Columbia University, NY, NY, 10027

Abstract

Since the early forties, one–point turbulence closure models have been the canonical tools used to describe turbulent flows in many fields. In geophysics, Mellor and Yamada applied such models using the 1980 state–of–the art. Since then, no improvements were introduced to alleviate two major difficulties: 1) closure of the pressure correlations, which affects the correct determination of the critical Richardson number Ri_{cr} above which turbulent mixing is no longer possible and 2) the need to express the non–local third–order moments (TOM) in terms of lower order moments rather than via the down–gradient approximation as done thus far, since the latter seriously underestimates the TOMs. Since 1) and 2) are still being dealt with adjustable parameters which weaken the credibility of the models, alternative models, not based on turbulence modeling, have been suggested.

The aim of this paper is to show that new information, partly derived from the newest 2–point closure model discussed in paper III, can be used to solve these shortcomings. The new one–point closure model, which in its simplest form is algebraic and thus simple to implement, is first shown to reproduce a variety of data. Then, it is used in a O–GCM where it reproduces well a large variety of ocean data.

While phenomenological models are specifically tuned to ocean turbulence, the present model is not. It is first tested against laboratory data on stably stratified flows and then used in an O–GCM. It is more general, more predictive and more resilient, e.g., it can incorporate phenomena like wave–breaking at the surface, salinity diffusivity, non–locality, etc. One important feature that naturally comes out of the new model is that the predicted Richardson critical value Ri_{cr} is $Ri_{cr}\sim 1$ in agreement with both LES and empirical evidence while all previous models predicted $Ri_{cr}\sim 0.2$ which led to a considerable underestimate of the extent of turbulent mixing and thus to an incorrect mixed layer depth. The predicted temperature and salinity profiles (vs. depth) are presented and compared with those of the KPP model and Levitus data.

I. Introduction

One–point closure turbulence models have a long tradition that begun with the pioneering work of Chou (1940, 1945) that was subsequently extended and improved by Lumley and Khajeh–Nouri (1974), Launder, Reece and Rodi (1975), Pope (1975), Lumley (1978), Rodi (1984) and Shih and Shabbir (1992). For a review, see Gatski et al., (1991). In a pioneering work, Mellor and Yamada (1982, MY; Mellor, 1989) applied the 1980 state–of–the–art 1–point closure models to geophysical problems. The original MY model is known for its successes and its failures: 1) *it does not parameterize the pressure correlations correctly.* This has two consequences: it predicts a critical Richardson number Ri_{cr}=0.2 (above which turbulence can no longer be maintained) that is much smaller than $Ri_{cr}\approx 1$ required by empirical evidence and LES (large eddy simulations, Wang et al, 1996), which means that the YM model underestimates the extent of turbulent mixing and given in correct mixed layer depth, second, the model does not fit the PBL surface data, 2) *it treats the third–order moments (TOM) with the down–gradient approximation* (DGA) which is now known to severely underpredict the true TOM. And yet, even the most recent applications of the MY model to ocean turbulence (e.g., Rosati and Miyakoda, 1989; Galperin et al., 1989; Gaspar et al., 1990; Blanke and Delecluse, 1992; Baum and Caponi, 1992; Ma et al., 1994; Kantha and Clayson, 1994; Burchard and Buamert, 1995; D'Alessio et al., 1998), still use the original model with changes that do not solve the difficulties 1) and 2). It is fair to say that, unless and until such shortcomings are solved, the credibility of the model is at stake. We have solved 1) and 2) as follows. Pressure correlations originate from the Navier–Stokes equations for the turbulent velocity field which contain the pressure gradients. For example, in deriving the equations for the Reynolds stresses and the heat fluxes, vectors and tensors appear which represent the correlation of fluctuating temperature and velocities with $p_{,i}$:

$$\Pi_i^{\theta} \equiv \overline{\theta p}_{,i} \qquad \Pi_{ij} \equiv \overline{u_j p}_{,i} + \overline{u_j p}_{,i} \tag{1}$$

where p, u_i and θ are the fluctuating components of the pressure, velocity and temperature fields. Since the fluctuating pressure p does not satisfy the hydrostatic equilibrium equation, these higher–order terms must be modeled in terms of second–order terms. As discussed in Appendix A, the most complete expressions are (for sake of simplicity, we leave out the numerical coefficients; all the tensors are defined in Appendix A)

$$\Pi_{ij} = 2\tau_{pv}^{-1} b_{ij} - \tfrac{4}{5} K S_{ij} + B_{ij} - \Sigma_{ij} - Z_{ij} \tag{2}$$

$$\Pi_i^{\theta} = \tau_{p\theta}^{-1} \overline{u_i \theta} + \lambda_i \overline{\theta^2} - (S_{ij} + \tfrac{5}{3} V_{ij}) \overline{u_j \theta} \tag{3}$$

The first terms in both 2) and 3) represent the return to isotropy or Rotta terms; the second and third terms in (2) are the contributions due to shear (S_{ij}) and buoyancy (B_{ij}); the fourth term is due to the non–isotropic contribution due to shear while the last term is entirely due to the vorticity V_{ij}. None of the second–order closure models employed thus far in O–GCM has employed the full form (2–3) and that is why these models often underestimate the true value of Ri_{cr}. For example, even the rather complete analysis by Kantha and Clayson (1994) adopts the simplified expressions

$$\Pi_{ij} = 2\tau_{pv}^{-1} b_{ij} - \tfrac{4}{5} K S_{ij}$$

$$\Pi_i^{\theta} = \tau_{p\theta}^{-1} \overline{u_i \theta} + \lambda_i \overline{\theta^2} - S_{ij} \overline{u_j \theta} \tag{4a}$$

which neglects the last three terms in Π_{ij}. The model of D'Alessio et al. (1998) adopts an even simpler expression:

$$\Pi_i^{\theta} = \tau_{p\theta}^{-1} \overline{u_i \theta} + \lambda_i \overline{\theta^2} \tag{4b}$$

which also neglects terms in Π_{ij} which we have found instrumental in the determination of Ri_{cr}. We have adopted the full forms (2)–(3).

The second problem concerns the pressure–temperature and the pressure–velocity time scales $\tau_{p\theta}$, τ_{pv}. Specifically, the question arises as how to evaluate the ratios

$$\tau_{p\theta}/\tau, \quad \tau_{pv}/\tau \tag{4c}$$

assuming that the dynamical time scale $\tau = 2K\epsilon^{-1}$ is known from solving the dynamic equations for K and ϵ. All one–point closure formalisms thus far have been unable to determine (4c) and empirical constants were thus introduced to represent $\tau_{p\theta}/\tau$ and τ_{pv}/τ.

These adjustable parameters weaken the credibility of the model. The two–point closure model discussed and employed in paper I has allowed us to determine such time scales whose values are no longer free. They are given by:

$$\frac{\tau_{pv}}{\tau} = \frac{2}{5}, \quad \frac{\tau_{p\theta}}{\tau} = \frac{1}{5}(1+\sigma_t^{-1})^{-1}, \quad \frac{\tau_\theta}{\tau} = \sigma_t \tag{4d}$$

where $\sigma_t = 0.72$ and where we have added the temperature variance ($\equiv\overline{\theta^2}$) dissipation time scale τ_θ. An immediate bonus of these improvements is that the new model matches the measured surface PBL data rather well:

Table I

	$\overline{u}^2/2K$	$\overline{v}^2/2K$	$\overline{w}^2/2K$	Ri(cr)
PBL data	0.56	0.27	0.18	0.5
MY Model	0.56	0.22	0.22	0.2
New model	0.56	0.27	0.18	0.5

Next, we discuss the problem of the third–order moments TOM which represent non–locality. The prototype is the flux of turbulent kinetic energy:

$$F(K) = \tfrac{1}{2}\overline{q^2 w}, \quad K = \tfrac{1}{2}\overline{q^2} \tag{5a}$$

All ocean turbulence models used thus far either disregard the TOM altogether (local model), or use the DGA which assumes that the kinetic energy flux is along the gradient of K:

$$F(K) = -K_m \frac{\partial K}{\partial z} \tag{5b}$$

However, as shown by Moeng and Wyngaard (1989), the DGA severely underestimates the true value of the TOM and thus, it should be avoided. All ocean turbulence models that employ a prognostic equation for K (Rosati and Miyakoda, 1989; Gaspar et al., 1990; Blanke and Delecluse, Ma et al., 1994) have adopted the DGA, (5b). In addition, the diffusivity K_m is taken proportional to $w\ell$: however, in the case of stratification, K_m is a combination of both the momentum and the heat fluxes,

$$K_m = aw\ell + b\overline{w\theta} \tag{5c}$$

and since for stably stratification, $\overline{w\theta}$ is negative, the second term decreases the diffusivity. Once the down–gradient approximation is abandoned, the only alternative is to consider the full dynamic equations for the third–order moments (Appendix B) and try to solve them. In the 1D case, this was done and the results are as follows (Canuto et al., 1994):

$$\begin{aligned}
\overline{q^2 w} &= E_1 \frac{\partial}{\partial z}\overline{w\theta} + E_2 \frac{\partial}{\partial z}\overline{w^2} + E_3 \frac{\partial}{\partial z}\overline{\theta^2} + E_4 \frac{\partial}{\partial z}\overline{q^2} \\
\overline{w^3} &= B_1 \frac{\partial}{\partial z}\overline{w\theta} + B_2 \frac{\partial}{\partial z}\overline{w^2} + B_3 \frac{\partial}{\partial z}\overline{\theta^2} + B_4 \frac{\partial}{\partial z}\overline{q^2} \\
\overline{w^2\theta} &= A_1 \frac{\partial}{\partial z}\overline{w\theta} + A_2 \frac{\partial}{\partial z}\overline{w^2} + A_3 \frac{\partial}{\partial z}\overline{\theta^2} + A_4 \frac{\partial}{\partial z}\overline{q^2} \\
\overline{w\theta^2} &= C_1 \frac{\partial}{\partial z}\overline{w\theta} + C_2 \frac{\partial}{\partial z}\overline{w^2} + C_3 \frac{\partial}{\partial z}\overline{\theta^2} + C_4 \frac{\partial}{\partial z}\overline{q^2} \\
\overline{q^2\theta} &= D_1 \frac{\partial}{\partial z}\overline{w\theta} + D_2 \frac{\partial}{\partial z}\overline{w^2} + D_3 \frac{\partial}{\partial z}\overline{\theta^2} + D_4 \frac{\partial}{\partial z}\overline{q^2} \\
\overline{\theta^3} &= F_1 \frac{\partial}{\partial z}\overline{w\theta} + F_2 \frac{\partial}{\partial z}\overline{w^2} + F_3 \frac{\partial}{\partial z}\overline{\theta^2} + F_4 \frac{\partial}{\partial z}\overline{q^2}
\end{aligned} \tag{5d}$$

Eqs.(5d) exhibit a remarkable symmetry: all the third–order moments have the same structure since they are linear combinations of the derivatives of all the second–order moments. Second, all the turbulent diffusivities A–F exhibit the same general structure (5c). The DGA corresponds to taking

$$\begin{aligned}
A_{2,3,4} &= 0,\ B_{1,3,4} = 0,\ C_{1,2,4} = 0 \\
D_{2,3,4} &= 0,\ E_{1,2,3} = 0,\ F_{1,2,4} = 0
\end{aligned} \tag{5e}$$

In Canuto et al. (1994) the new TOM (5d) were tested against large eddy simulation data for the PBL. The results were quite good. Eqs.(5d) are the most complete representation of the TOM presently available.

Finally, we discuss the dissipation length scale. The dissipation rate ϵ of the turbulent kinetic energy K is one of the most crucial and most difficult variables to model. Although an exact differential equation for ϵ was derived long ago, it has been used only very seldom (e.g., Burchard and Buamert, 1995). Most frequently, use is made of the local form:

$$\epsilon = \ell^{-1} K^{3/2} \tag{5f}$$

The problem then reduces to the evaluation of the dissipation length scale ℓ. Until recently, several empirical expressions for ℓ have been proposed which often seem to contradict each other. Among these formulae, the most widely used are the ones due to Deardorff (1980) which includes only buoyancy, and by Hunt et al. (1988) which includes only shear. Neither expression is valid in the limit of small buoyancy or shear. Starting from a theoretical formulation of the buoyancy spectrum in stably stratified flow due to Lumley (1964) and Weinstock (1978), a new expression was derived for ℓ that: a) includes both buoyancy and shear, b) encompasses all previous models of ℓ, c) behaves well for small buoyancy and/or shear, and d) explains the non–monotonic behavior of ℓ found by LES.

In conclusion, we show that a one–point closure model free of the uncertainties of the past can be constructed. Tests of the model are presented before being used in an O–GCM, the results of which are also presented. On the basis of its overall performance, the model will be further expanded to include salinity (paper II).

III. Turbulence model

We begin by recalling that in an ocean GCM the equations for the mean velocity and mean temperature entail the Reynolds stresses $\overline{u_i u_j}$ and the heat fluxes h_i

$$\tau_{ij} = \overline{u_i u_j}, \qquad h_i = \overline{u_i \theta} \tag{6a}$$

where u_i and θ are the fluctuating components of the velocity and temperature fields. The well established procedure of deriving the dynamic equations for the variables (1a) entails other turbulence variables, specifically (ν and χ are the kinematic viscosity and thermal conductivity):

$$K \equiv \tfrac{1}{2}\tau_{ii} \text{ (turbulent kinetic energy)} \tag{6b}$$

$$\overline{\theta^2} = \text{(temperature variance)} \tag{6c}$$

$$\epsilon = \nu \overline{\left(\frac{\partial u_i}{\partial x_j}\right)^2} \text{ (dissipation rates of K)} \tag{6d}$$

$$\epsilon_\theta = \chi \overline{\left(\frac{\partial \theta}{\partial x_i}\right)^2} \text{ (dissipation rates of } \overline{\theta^2}) \tag{6e}$$

There are a total of 12 independent variables, each of which satisfies a separate dynamic equation, and each of which depends on the others so that it is not possible to derive the heat flux without solving the equation for the Reynolds stresses and viceversa. Since the derivation of the dynamic equations for the turbulence variables (6a–e) has been presented elsewhere (e.g., Gatski et al., 1991; Canuto, 1994), we shall only cite the results.

a) Turbulent kinetic energy K:

$$\frac{DK}{Dt} + D_f(K) = P_s + P_b - \epsilon \tag{7a}$$

where the production terms P's due to shear and buoyancy are defined as

$$P_s \equiv -\tau_{ij} S_{ij}, \qquad P_b \equiv \lambda_i h_i, \tag{7b}$$

while the divergence of flux of turbulent kinetic energy $F_i(K)$ is given by

$$D_f(K) \equiv \frac{\partial}{\partial x_i} F_i(K), \qquad F_i(K) = \tfrac{1}{2}\rho \overline{q^2 u_i} \tag{7c}$$

Finally, $\lambda_i \equiv g_i \alpha_T$ with $g_i=(0,0,g)$ and $\alpha_T = -\rho^{-1}\partial\rho/\partial T$. The shear S_{ij} is defined in Eq.(A.6)

b) Temperature variance (potential energy) $\overline{\theta^2}$:

$$\frac{D}{Dt}\tfrac{1}{2}\overline{\theta^2} + D_f(\tfrac{1}{2}\overline{\theta^2}) = P_\theta - \epsilon_\theta + \tfrac{1}{2}\chi \frac{\partial^2}{\partial x_i^2}\overline{\theta^2} \tag{8a}$$

$$P_\theta = -h_i \frac{\partial T}{\partial x_i}, \qquad D_f(\tfrac{1}{2}\overline{\theta^2}) = \tfrac{1}{2}\frac{\partial}{\partial x_i}(\overline{u_i \theta^2}) \tag{8b}$$

P_θ and D_f represent the rates of production and transport of the divergence of the flux of temperature variance and ϵ_θ represents the rate of dissipation of $\frac{1}{2}\overline{\theta^2}$, Eq.(6e).

c) Reynolds stresses, $b_{ij} \equiv \tau_{ij} - \frac{2}{3} K \delta_{ij}$:

$$\frac{D}{Dt} b_{ij} + D_f(b_{ij}) = -\frac{8}{15} K S_{ij} - 2\tau_{pv}^{-1} b_{ij} + \beta_5 B_{ij} - (1-\alpha_1)\Sigma_{ij} - (1-\alpha_2) Z_{ij} \tag{9a}$$

The traceless tensors **B**, **Σ** and **Z** are defined as

$$B_{ij} = \lambda_i h_j + \lambda_j h_i - \frac{2}{3}\delta_{ij}\lambda_k h_k \tag{9b}$$

$$\Sigma_{ij} = S_{ik}b_{kj} + S_{jk}b_{ik} - \frac{2}{3}\delta_{ij}S_{k\ell}b_{k\ell} \tag{9c}$$

$$Z_{ij} = V_{ik}b_{kj} + V_{jk}b_{ik} \tag{9d}$$

Shear S_{ij} and vorticity V_{ij} are defined as:

$$S_{ij} = \tfrac{1}{2}\left(\frac{\partial U_i}{\partial x_j} + \frac{\partial U_j}{\partial x_i}\right), \qquad V_{ij} = \tfrac{1}{2}\left(\frac{\partial U_i}{\partial x_j} - \frac{\partial U_j}{\partial x_i}\right) \tag{9e}$$

The diffusion term is defined as

$$D_f(b_{ij}) = \frac{\partial}{\partial x_k}\left(\overline{u_i u_j u_k} - \frac{1}{3}\delta_{ij}\overline{q^2 u_k}\right) \tag{9f}$$

c) Heat flux: $h_i = \overline{u_i \theta}$

$$\frac{D}{Dt}h_i + D_f(h_i) = -\tau_{ij}\frac{\partial T}{\partial x_j} - \left(1 - \frac{3}{4}\alpha_3\right)h_j S_{ij} - \left(1 - \frac{5}{4}\alpha_3\right)h_j V_{ij} + (1-\gamma_1)\lambda_1 \overline{\theta^2} - \tau_p^{-1}h_i + \chi\frac{\partial^2}{\partial x_j^2}h_i \tag{10a}$$

where

$$D_f(h_i) = \frac{\partial}{\partial x_j}\left(\overline{u_i u_j \theta} + \delta_{ij}\overline{p\theta}\right) \tag{10b}$$

d) Dissipation rate ϵ_θ:

$$\epsilon_\theta = \tau_\theta^{-1}\overline{\theta^2} \tag{11}$$

e) Dissipation rate ϵ:

$$\frac{D\epsilon}{Dt} + D_f(\epsilon) = \epsilon K^{-1}(c_1 P_s + c_3 P_b) - c_2 \epsilon^2 K^{-1} \tag{12a}$$

$$D_f(\epsilon) = \frac{\partial}{\partial x_i}\left(\overline{\epsilon u_i}\right) \tag{12b}$$

Since we have assumed an algebraic for ϵ_θ, the number of dynamic equations is now 11.

IV. Diffusion terms D_f

The third–order moments are discussed in Appendix B.

V. Algebraic Models

The above model is complete and allows us to compute the turbulent variables of interest. In its full dynamical form, it is obviously rather complex since it entails 11

differential equations. In this section, we present a model in which we retain only two of the eleven differential equations, those for K and ϵ. The procedure, known as ARSM, *algebraic Reynolds stress models*, neglects the D/Dt and the diffusion terms. After some algebra, we obtain:

Reynolds Stresses:

$$b_{ij} = -\frac{4}{15}K\tau_{pv}S_{ij} + \tfrac{1}{2}\beta_5\tau_{pv}B_{ij} - \tfrac{1}{2}\tau_{pv}(1-\alpha_1)\Sigma_{ij} - \tfrac{1}{2}\tau_{pv}(1-\alpha_2)Z_{ij} \qquad (13)$$

Since the last two terms depend on b_{ij} itself, Eq.(13)is a system of linear algebraic equations.

Heat fluxes:

$$A_{ik}h_k = -(K_h)_{ij}\frac{\partial T}{\partial x_j} \qquad (14a)$$

where the turbulent heat conductivity tensor is given by

$$(K_h)_{ij} = \tau(b_{ij} + \frac{2}{3}\delta_{ij}K), \qquad \tau = 2K\epsilon^{-1} \qquad (14b)$$

The dimensionless tensor A_{ij} is defined as:

$$A_{ij} = \frac{\tau}{\tau_{p\theta}}\delta_{ij} + (1-\gamma_1)\tau\tau_\theta\lambda_i\frac{\partial T}{\partial x_j} + (1-\frac{3}{4}\alpha_3)\tau S_{ij} + (1-\frac{5}{4}\alpha_3)\tau V_{ij} \qquad (14c)$$

The fact that the rhs of (14b) depends on b_{ij} which in turn depends on h_i via B_{ij} makes the analytic solution in the 3D case somewhat cumbersome though manageable with symbolic algebra. In order to homogenize the notation, we introduce the dimensionless constants:

$$\lambda = \frac{\tau_{pv}}{\tau}, \quad \lambda_1 = \frac{4}{15}\lambda, \quad \lambda_2 = \tfrac{1}{2}(1-\alpha_1)\lambda, \quad \lambda_3 = \tfrac{1}{2}(1-\alpha_2)\lambda, \quad \lambda_4 = \tfrac{1}{2}\beta_5\lambda$$

$$\lambda_5 = \frac{\tau}{\tau_{p\theta}}, \quad \lambda_6 = 1-\frac{3}{4}\alpha_3, \quad \lambda_7 = 1-\frac{5}{4}\alpha_3, \quad \lambda_8 = (1-\gamma_1)\frac{\tau_\theta}{\tau} \qquad (14d)$$

Thus, Eqs.(13) and (14c) can be written in the compact form:

$$b_{ij} = -\lambda_1\tau KS_{ij} + \lambda_4\tau B_{ij} - \lambda_2\tau\Sigma_{ij} - \lambda_3\tau Z_{ij} \qquad (14e)$$

$$A_{ij} = \lambda_5\delta_{ij} + \lambda_8\tau^2\lambda_i\frac{\partial T}{\partial x_j} + \lambda_6\tau S_{ij} + \lambda_7\tau V_{ij} \qquad (14f)$$

VI. Vertical Diffusivities

Here, we present the analytic solution of Eqs. (13)–(14) for the following case:

$$\frac{\partial T}{\partial x_i} \to \frac{\partial T}{\partial z}\,\delta_{i3}, \qquad U_i = [U(z),\, V(z),\, 0] \tag{15a}$$

The shear and vorticity acquire the form:

$$S_{ij}=\tfrac{1}{2}\begin{bmatrix} 0 & 0 & \partial U/\partial z \\ 0 & 0 & \partial V/\partial z \\ \partial U/\partial z & \partial V/\partial z & 0 \end{bmatrix}, \qquad V_{ij}=\tfrac{1}{2}\begin{bmatrix} 0 & 0 & \partial U/\partial z \\ 0 & 0 & \partial V/\partial z \\ -\partial U/\partial z & -\partial V/\partial z & 0 \end{bmatrix} \tag{15b}$$

Using symbolic algebra, one can solve Eqs.(14a,b,e, f). The results are as follows:

Reynolds stresses:

$$\overline{uw} = -K_m\frac{\partial U}{\partial z},$$

$$\overline{vw} = -K_m\frac{\partial V}{\partial z} \tag{16a}$$

$$\overline{uv} = (\lambda_2+\lambda_3)\tau K_m\frac{\partial U}{\partial z}\frac{\partial V}{\partial z} \tag{16b}$$

Time scale:

$$\tfrac{1}{2}\tau = \frac{K}{\epsilon} \tag{17}$$

Turbulent kinetic energies:

$$\overline{u^2} = \frac{2}{3}K + \frac{1}{3}\tau K_m[(\lambda_2+3\lambda_3)(\frac{\partial U}{\partial z})^2 - 2\lambda_2(\frac{\partial V}{\partial z})^2] + \frac{2}{3}\lambda_4 K_h \tau N^2 \tag{18a}$$

$$\overline{v^2} = \frac{2}{3}K + \frac{1}{3}\tau K_m[(\lambda_2+3\lambda_3)(\frac{\partial V}{\partial z})^2 - 2\lambda_2(\frac{\partial U}{\partial z})^2] + \frac{2}{3}\lambda_4 K_h \tau N^2 \tag{18b}$$

$$\overline{w^2} = \frac{2}{3}K + \frac{1}{3}(\lambda_2-3\lambda_3)K_m\tau\Sigma^2 - \frac{4}{3}\lambda_4 K_h\tau N^2 \tag{18c}$$

Mean shear:

$$\Sigma^2 \equiv (\frac{\partial U}{\partial z})^2+(\frac{\partial V}{\partial z})^2 \tag{18d}$$

Heat fluxes:

$$\overline{w\theta} = -K_h\frac{\partial T}{\partial z} \tag{19a}$$

$$\overline{u\theta} = -\lambda_5^{-1}[K_m+\tfrac{1}{2}(\lambda_6+\lambda_7)K_h]\tau\frac{\partial T}{\partial z}\frac{\partial U}{\partial z} \tag{19b}$$

$$\overline{v\theta} = -\lambda_5^{-1}[K_m+\tfrac{1}{2}(\lambda_6+\lambda_7)K_h]\tau\frac{\partial T}{\partial z}\frac{\partial V}{\partial z} \tag{19c}$$

Turbulent momentum and heat diffusivities:

$$K_m = 2S_m\frac{K^2}{\epsilon}, \qquad K_h = 2S_h\frac{K^2}{\epsilon} \tag{20a}$$

As discussed in I, the dimensionless structure functions $S_{m,h}$ are instrumental in

being able to show that the model satisfies a well known feature of stably stratified flows (Webster, 1964), namely that the turbulent Prandtl number

$$\sigma_T = \frac{K_m}{K_h} \tag{20b}$$

is an increasing function of the Richardson number Ri:

$$\frac{d}{dRi}\,\sigma_T(Ri) > 0, \qquad Ri \equiv \frac{g\alpha\partial T/\partial z}{\Sigma^2} \tag{20c}$$

The function $\sigma_T(Ri)$ vs. Ri will be discussed in sec. XVIII.

VII. Structure Functions

Dimensionless functions $S_{m,h}$:

$$DS_m = s_0 + s_1(\tau N)^2 + s_2(\tau\Sigma)^2 \tag{21a}$$

$$DS_h = s_4 + s_5(\tau N)^2 + s_6(\tau\Sigma)^2 \tag{21b}$$

$$D = d_0 + d_1(\tau N)^2 + d_2(\tau\Sigma)^2 + d_3(\tau N)^4 + d_4(\tau^2 N\Sigma)^2 + d_5(\tau\Sigma)^4 \tag{21c}$$

Plots of $S_{m,h}$ vs. Ri will be exhibited in sec.XVIII.

Dimensionless variables s_k:

$$s_0 = \frac{3}{2}\lambda_1\lambda_5^2 \tag{22a}$$

$$s_1 \equiv -\lambda_4(\lambda_6+\lambda_7) + 2\lambda_4\lambda_5(\lambda_1 - \tfrac{1}{3}\lambda_2 - \lambda_3) + \frac{3}{2}\lambda_1\lambda_5\lambda_8 \tag{22b}$$

$$s_2 \equiv -\frac{3}{8}\lambda_1(\lambda_6^2-\lambda_7^2), \quad s_4 \equiv 2\lambda_5, \quad s_5 = 2\lambda_4 \tag{23a}$$

$$s_6 = \frac{2}{3}\lambda_5(3\lambda_3^2-\lambda_2^2) - \tfrac{1}{2}\lambda_5\lambda_1(3\lambda_3-\lambda_2) + \frac{3}{4}\lambda_1(\lambda_6-\lambda_7) \tag{23b}$$

Dimensionless variables d_k:

$$d_0 = 3\lambda_5^2 \tag{24a}$$

$$d_1 \equiv \lambda_5(7\lambda_4 + 3\lambda_8), \quad d_2 \equiv \lambda_5^2(3\lambda_3^2-\lambda_2^2) - \frac{3}{4}(\lambda_6^2-\lambda_7^2) \tag{24b}$$

$$d_3 \equiv \lambda_4(4\lambda_4 + 3\lambda_8), \quad d_5 \equiv \frac{1}{4}(\lambda_2^2 - 3\lambda_3^2)(\lambda_6^2-\lambda_7^2) \tag{24c}$$

$$d_4 \equiv \lambda_4[\lambda_2\lambda_6 - 3\lambda_3\lambda_7 - \lambda_5(\lambda_2^2-\lambda_3^2)] + \lambda_5\lambda_8(3\lambda_3^2-\lambda_2^2) \tag{24d}$$

As a way of comparison with recent work, we notice that the expressions for $\overline{uw}$ and $\overline{w\theta}$ employed by D'Alessio et al. (1998, see equations 6–12) are equivalent to taking $\Sigma \to 0$, that is, their diffusivities do not depend on the source (shear). In that case our S_m would

become a constant

$$S_m = 0.09 \tag{24e}$$

As we shall show, in our model this value corresponds to $Ri \leq 0$, whereas one expects that S_m decreases with Ri for the reasons given above.

Since in the above relations K and ϵ have remained unspecified, one can choose different models.

VIII. First non–local model.

In this case K and ϵ are taken to satisfy the two non–local equations:

$$\frac{DK}{Dt} + D(K) = K_m\Sigma^2 - K_h N_h^2 - \epsilon \tag{25a}$$

$$\frac{D\epsilon}{Dt} + D(\epsilon) = \epsilon K^{-1}(c_1 K_m\Sigma^2 - c_3 K_h N_h^2) - c_2\epsilon^2 K^{-1} \tag{25b}$$

This type of model was adopted by Baum and Caponi (1992), Kantha and Calyson (1994) and Burchard and Baumert (1995).

IX. Second non–local model.

In this case, one retains only one prognostic equation, the one for the turbulent kinetic energy K, Eq.(25a), while Eq.(25b) is taken in its local limit

$$\epsilon = \Lambda^{-1}K^{3/2} \tag{25c}$$

where the mixing length Λ has to be specified. Models of this type with down–gradient approximation for the diffusion term were considered by Rosati and Miyakoda (1989), Gaspar et al. (1990), Blanke and Delecluse (1993) and Ma et al. (1994).

X. Third non–local model

In this model, Eq.(25a) is taken in its local form by neglecting the left hand side altogether while one retains Eq.(26) so as to avoid the need to introduce a mixing length ℓ. The local limit of (25a) is physically equivalent to assuming production=dissipation,

$$\epsilon = K_m\Sigma^2 - K_h N^2 \tag{26a}$$

or, using the relation $\tau=2K\epsilon^{-1}$,

$$(\tau\Sigma)^2 S_m - (N_h\tau)^2 S_h = 2 \tag{26b}$$

Using Eqs.(22a–c), Eq.(26b) becomes an equation for the dimensionless variable

$$(\tau\Sigma)^2 \equiv \psi \tag{26c}$$

The result is:

$$A\psi^2 + B\psi + C = 0 \tag{26d}$$

$$A \equiv (s_5+2d_3)Ri^2 - (s_1-s_6-2d_4)Ri - s_2 + 2d_5$$

$$B = (s_4+2d_1)Ri - s_0 + 2d_2, \quad C = 2d_0 \tag{26e}$$

The function ψ vs. Ri will be discussed in sec. XVIII.

XI. Fully local model

In this case, both Eqs.(25) are taken to be local; K can then be expressed as

$$\frac{K}{K_0} = \psi^{-1}, \qquad K_0 = 4\Lambda^2\Sigma^2 \tag{27}$$

Once a model for Λ is provided, the model becomes fully algebraic.

XII. The critical Richardson number

The critical Richardson number Ri_{cr} is defined as the value of Ri above which turbulent mixing is no longer possible due to the action of stable stratification. While linear analysis yields the result $Ri_{cr}=1/4$ (Maslowe, 1981), it has been found (Martin, 1985) that a reliable prediction of the mixed layer depth can only be achieved if $Ri_{cr}\sim1$. Early laboratory data by Taylor (cited in Monin and Yaglom 1971) indicate that turbulent exchange exists even when Ri>1. In addition, recent LES studies (Wang et al., 1997) also show that turbulence exists up to Ri~1. This is therefore a critical test of any turbulence model. As discussed earlier, the original MY model gives an $Ri_{cr}=0.2$ which is even smaller than the result of the linear stability analysis, $Ri_{cr}=1/4$. We shall define Ri_{cr} as the value at which the kinetic energy vanishes:

$$K(Ri_{cr})=0 \tag{28a}$$

Since $\psi \sim K^{-1}$, Eq.(26d) implies that in the limit $K \to 0$, $A(Ri_{cr})=0$ which in turn gives

$$Ri_c = (2c_1)^{-1}[-c_2 + (c_2^2 - 4c_1 c_3)^{\frac{1}{2}}]$$

$$c_1 = s_5 + 2d_3, \quad c_2 = -s_1 + s_6 + 2d_4, \quad c_3 = -s_2 + 2d_5 \tag{28b}$$

Using the model constants discussed below,

$$Ri_c = 0.846 \text{ (model A)}$$

$$Ri_{cr} = 1.03 \text{ (model B)} \tag{28c}$$

in agreement with the data referred to earlier.

XIII. Realizability Conditions

Since by definition $(\tau\Sigma)^2>0$, from Eq.(26b) it follows that the minimum value of τN is

$$(\tau N)^2_{min} = -2S_h^{-1} \tag{29a}$$

or, using (21b) and the model constants, we derive:

$$(\tau N)^2_{min} = -12.27 \tag{29b}$$

The negative value of $(\tau N)^2_{min}$ means that it occurs in the unstable region. In the stable region, $(\tau N)^2$ is limited by stable stratification as follows (Deardorff, 1980)

$$(\tau N)^2_{max} = 4.66 \tag{29c}$$

On the other hand, by arguing that an increase of shear should not result in a decrease of $-\overline{uw}$, one can derive an expression for the maximum value for $(\tau\Sigma)^2$:

$$(\tau\Sigma)^2_{max} \approx [d_0 + d_1(\tau N)^2 + d_3(\tau N)^4][d_2 + d_4(\tau N)^2]^{-1} \tag{29d}$$

In applying the model, we shall use the following realizability conditions:

$$\begin{aligned} (\tau N)^2 &= (\tau N)^2_{min} && \text{if } (\tau N)^2 < (\tau N)^2_{min} \\ (\tau N)^2 &= (\tau N)^2_{max} && \text{if } (\tau N)^2 > (\tau N)^2_{max} \\ (\tau\Sigma)^2 &= (\tau\Sigma)^2_{max} && \text{if } (\tau\Sigma)^2 > (\tau\Sigma)^2_{max} \end{aligned} \tag{29e}$$

XIV. The representation $K_h = \gamma\epsilon N^{-2}$

Several authors (Thorpe, 1977; Osborne, 1980; Oakey, 1982; Moum, 1989; Davis et al.,

1994; Toole et al., 1994; Wuest et al., 1996) have represented the turbulent heat diffusivity K_h in the form:

$$K_h = \gamma \frac{\epsilon}{N^2} \tag{30a}$$

The derived values of γ are:

$$0.12 \leq \gamma \leq 0.48 \tag{30b}$$

Using (26a), we obtain:

$$\gamma = \frac{R_f}{1-R_f}, \quad R_f = Ri\ \sigma_T^{-1} \tag{30c}$$

where use must be made of (20b). The function $\gamma(Ri)$ vs. Ri is discussed in sec.XVIII. The value $\gamma=1/4$ (e.g., Oakey 1982; Toole et al., 1994) occurs at Ri=0.25. In using (30a), care must be exercised here since in general the heat diffusivity K_h is not the same as the "mass diffusivity" K_ρ defined via the relation:

$$\overline{\rho' w''} = -K_\rho \frac{\partial \rho}{\partial z} \tag{31a}$$

It is easy to derive the relation

$$K_\rho = K_h(1-\frac{K_s}{K_h} R_\rho)(1-R_\rho)^{-1}, \qquad R_\rho = \frac{\alpha_S}{\alpha} \frac{\partial S/\partial z}{\partial T/\partial z} \tag{31b}$$

where K_s is the salt diffusivity and R_ρ is the Turner number (α_s is the haline contraction coefficient). As in the present case, $K_s=K_h$, it follows that $K_h=K_\rho$.

XV. Breaking Waves

It has been known for a number of years (Kitaigorodskii et al., 1983; Gargett, 1989; Agrawal et al., 1992; Anis and Moum, 1994; Drennan et al., 1996; Terray et al., 1996, 1997; Burgers, 1997; Skyllingstad et al., 1999) that in the ocean mixed layer beneath actively breaking waves the dissipation rate ϵ of turbulent kinetic energy K is even two orders of magnitude larger than the one corresponding to the "law of the wall":

$$\epsilon_{wall} = u_*^3(\kappa z)^{-1}, \quad u_* = (\tau/\rho_w)^{\frac{1}{2}} \tag{32a}$$

which can be derived from (27). Here, where $\kappa \sim 0.4$ is the von Karman constant, z is the distance from the "wall", τ is the surface wind stress and ρ_w is the density of seawater. To

incorporate the wave breaking phenomenon into a turbulence model, one needs to solve the dynamic equation for the turbulent kinetic energy, Eq.(25). This in turn requires that a boundary condition to specify K at z=0. Craig and Banner (1994) first proposed the expression ($K\equiv\frac{1}{2}q^2$)

$$q|_{z=0} = (12c_1^{-1})^{1/6}\, u_*^{2/3}\, \bar{c}^{-1/3} \tag{32b}$$

where $\bar{c}$ is the "effective phase speed" (Terray et al., 1996) that enters the rate of energy input to the waves from the wind, $F=\tau_a\bar{c}/\rho_w \sim u_{*w}^2\bar{c}\equiv\alpha u_{*w}^3$, where $\tau_a=\rho_a u_{*a}^2=\rho_w u_{*w}^2$ (a:atmosphere, w:water). Craig and Banner (1994; their equation 27) use α rather than $\bar{c}$. The coefficient $c_1=0.18$. In Appendix C we present a new and simpler derivation of (32b) and in sec.XVIII we discuss the results of our model with breaking waves.

XVI. Modeling the length scale Λ

We begin by writing Λ that appears in (25c) as

$$\Lambda = c_\epsilon^{-1}\Delta f(N,\Sigma) \tag{33a}$$

and require that f(0,0)=1. Here, Δ is the size of the largest eddy, $k_0\Delta=\pi$ while $f(N,\Sigma)$ represents the distortion of the Kolmogorov spectrum due to stratification and shear. Though a satisfactory theory of the energy spectrum E(k) under shear and stable stratification is still not available, there is some consensus (Gargett et al., 1981) about the overall shape of E(k):

$$\begin{aligned}
&\text{I:} && E(k)=(\epsilon N)^{\frac{1}{2}}k^{-2}, && Fr<1,\ Ri>1\\
&\text{II:} && E(k)=cN^2k^{-3}, && Fr=1,\ Ri\sim 1\\
&\text{III:} && E(k)=Ko\epsilon^{2/3}k^{-5/3}, && Fr>1,\ Ri<1
\end{aligned} \tag{33b}$$

where Fr is the Froude number

$$Fr = \frac{K^{\frac{1}{2}}}{\Lambda N} \tag{33c}$$

For the ocean $c\approx 10$ (Gargett et al., 1981; Gargett 1989), while atmospheric data suggest $c\approx 100$ (Dewan, 1979) so that the interval between regimes I and II may be one or two

decades. Regions II and III coincide at a length scale given by the Ozmidov scale,

$$\Lambda_0 = \frac{K^{\frac{1}{2}}}{N} = \left(\frac{\epsilon}{N^3}\right)^{\frac{1}{2}} \tag{33d}$$

Deardorff (1980), Hunt et al. (1988) and Fernando and Hunt (1996) have suggested the following phenomenological relations:

$$f(N,0) = 0.76\,\frac{K^{\frac{1}{2}}}{\Delta N}, \qquad f(0,\Sigma) = 2.76\,\frac{K^{\frac{1}{2}}}{\Delta \Sigma} \tag{33e}$$

Deardorff's result, the first of (33e), comes from substituting Eq.(27) in the Ozmidov scale. Neither expression satisfies the condition f(0,0)=1 and thus they have a limited validity. Furthermore, f(N,0) implies that

$$\tau \sim \frac{K}{\epsilon} \sim \Lambda K^{-\frac{1}{2}} \sim N^{-1}, \quad \tau N \sim \text{constant} \tag{33f}$$

which in turn implies that

$$\psi = (\tau\Sigma)^2 \sim Ri^{-1} \tag{33g}$$

while (28d) implies the opposite, namely a ψ that increases with Ri. Similar remarks are valid for the second of (33e). There have been several attempts to construct a model for E(k,N,Σ). Lumley's (1964) model implies a function f(N,Σ) of the form (Cheng and Canuto, 1994):

$$f(N,\Sigma) = [1 - c_1 Fr^{-2}(1 - c_2 \sigma_T Ri^{-1})]^{-3/2} \tag{34a}$$

where $\sigma_T = \sigma_T(Ri)$. The two constants are given by

$$c_1 \equiv (2\pi^2 3^{\frac{1}{2}})^{-1} Ko^{3/2}, \quad c_2 = 0.4\text{–}0.6 \tag{34b}$$

As discussed in Cheng and Canuto (1994), Lumley's formulation is valid only for small levels of stratification. Weinstock (1978) suggested an improvement of Lumley's model and the corresponding form of f(N,S) is (Cheng and Canuto 1994):

$$f(N,\Sigma) = [(1-A^2B^2)^{\frac{1}{2}} - AC]^{-3} \tag{34c}$$

where

$$A \equiv a_1(1 - c_2 \sigma_T Ri^{-1}), \quad B^{-1} = a_2 + Fr^2, \quad C^{-1} = a_3 + Fr^2$$
$$a_1 = 8.6810^{-3} Ko^{3/2}, \; a_2 = \frac{5}{2}10^{-2}, \; a_3 = \frac{3}{2}\,10^{-2} \tag{34d}$$

Recently, Cheng and Canuto (1994) improved on both Lumley and Weinstock's model and

checked the result against LES data (see their Fig.5). The function $f(N,\Sigma)$ is given by:

$$f(N,\Sigma) = [1 + aFr^{-2}(1+bFr^{-4/3})^{-1}]^{-c} \tag{34e}$$

where

$R_f<c_2$:

$$a = 2(3\pi^2)^{-1}(\Omega-1),\ b = 0.12\ (\Omega - 1 - \tfrac{3}{2}\Omega^{-1})^{4/9},\ c = \frac{3}{2} \tag{34f}$$

$R_f>c_2$:

$$a = 4(5\pi^2)^{-1}\Omega,\ b=0,\ c = \frac{5}{4}(1-\Omega^{-1})$$

$$\Omega = 1 + \frac{3^{\frac{1}{2}}}{4} Ko^{3/2}(\sigma_T Ri^{-1} - 1) \tag{34g}$$

Canuto and Cheng (1997) have further improved on their original model and their new expression for $f(N,\Sigma)$ is Equation (6a) of that paper. In the case in which one considers only shear, $f(0,\Sigma)$ simplifies considerably:

$$2f^{-2/3} = 1 + pSh^2 + (1 + 2pSh^2 - \tfrac{4}{5}p^2Sh^4)^{\frac{1}{2}} \tag{34h}$$

where

$$Sh \equiv \Delta\Sigma K^{-\frac{1}{2}},\quad p=\frac{1}{8}(2\pi^2 3^{\frac{1}{2}})^{-1}Ko^{3/2} \tag{34i}$$

In the simplest model, Λ is determined using the Deardorff–Blackadar formula:

$$\Lambda = 2^{-3/2}B_1\ell,\qquad B_1=24.7,$$

$$\ell = \min(\tfrac{1}{2}\frac{q}{N},\ \ell_1) \tag{34j}$$

$$\ell_1 = \kappa z\ell_0(\ell_0+\kappa z)^{-1},\qquad \ell_0 = 0.17H \tag{34k}$$

where $\frac{1}{2}q^2=K$ is the turbulent kinetic energy, N is the Brunt–Vaisala frequency, $\kappa=0.4$ is the von Karman constant and H is the mixed layer depth. When used within the NCAR CSM Ocean Model, H is determined as the depth where the buoyancy difference

$$g[\rho(H)-\rho(\text{surface})]\rho(H)^{-1} = 3\ 10^{-4}ms^{-2} \tag{34ℓ}$$

XVII. Model constants

As discussed in the Introduction, we use the new two–point closure turbulence model discussed in paper I to determine the critical time scales. The results are:

$$\tau_{pv}\tau^{-1} = \frac{2}{5}, \quad \tau\tau_{p\theta}^{-1} = 5(1+\sigma_t^{-1}), \quad \tau_\theta\tau^{-1} = \sigma_t$$

$$\sigma_t=0.72, \quad \gamma_1=\frac{1}{3}, \quad \beta_5=0.6,$$

$$10\alpha_5=1+\frac{4}{5}F^{\frac{1}{2}}, \quad \alpha_1=6\alpha_5, \quad \frac{3}{2}\alpha_2=2-7\alpha_5, \quad \alpha_3=\frac{4}{5}, \quad F=0.64 \tag{35a}$$

The values of the λ's defined in Eq.(14d) are then as follows:

Model A:

$$(\lambda_1,\lambda_2,\lambda_3,\lambda_4,\lambda_5,\lambda_6,\lambda_7,\lambda_8)=$$

$$(0.107,\ 0.0032,\ 0.0864,\ 0.12,\ 11.9,\ 0.4,\ 0,\ 0.48) \tag{35b}$$

The corresponding Ri_{cr} is:

$$Ri_{cr}= 0.846 \tag{35c}$$

which is more than four times larger than the MY result. On the other hand, to lend further support to the turbulence model that led us to (35b), we have devised an alternative procedure (Appendix D) which is based on entirely different considerations and which gives very similar results:

Model B:

$$(\lambda_1,\lambda_2,\lambda_3,\lambda_4,\lambda_5,\lambda_6,\lambda_7,\lambda_8)=$$

$$(0.127,\ 0.00336,\ 0.0906,\ 0.101,\ 11.2,\ 0.4,\ 0,\ 0.318) \tag{35d}$$

with Ri_{cr}:

$$Ri_{cr} = 1.03 \tag{35e}$$

In the first model, we have also used data from Shih and Shabbir (1992).

XVIII. Tests of the model

We begin with the case of pure shear, Ri→0, which has been widely studied. In this case, we have (to first order) from (21a,c)

$$DS_m = s_0, \quad D = d_0, \quad S_m= \frac{4}{75} \tag{36a}$$

Thus, the first of (20a) becomes

$$K_m = C_\mu \frac{K^2}{\epsilon}, \quad C_\mu=0.11 \tag{36b}$$

which is the well known formula employed in shear flows studies (Rodi, 1984).

In Fig.1 we exhibit the dimensionless structure functions $S_{m,h}$ vs. Ri for the full local model, Eqs.(21a,c) and (26d). The left hand side of the figure is for unstable stratification (Ri<0) while the right hand panel is for stable stratification, Ri>0. As one can expect, the relative position of the curves switches as one moves from negative to positive Ri. In the unstable case, the heat diffusivity is larger than the momentum diffusivity since one expects that the temperature gradient affects more the heat diffusivity than the momentum diffusivity. The reverse is true when stratification is stable. The lower value of S_h vs. S_m is in accord with the laboratory data for the turbulent Prandtl number which we discuss below. In Fig.2 we exhibit the dynamical time scale τ in units of the shear Σ vs. Ri, that is the function ψ(Ri), Eq.(26c), which is solution of Eq.(26d). As expected, the stronger the stratification, the longer is the eddies life time, or equivalently, the smaller the turbulent kinetic energy, since $\psi \sim K^{-1}$. In Fig.3 we report the laboratory data for σ_T vs. Ri by Webster (1964) and in Fig.4 we exhibit the predicted turbulent Prandtl number σ_T vs. Ri, Eqs.(20b) and (21). In Fig.5 we show the predicted flux Richardson number R_f vs. Ri defined in Eq.(30c). In Fig.6, we present a set of laboratory data for R_f vs. Ri from the work of Maderich et al. (1995). Since the definitions of the Richardson numbers in Figs.5 and 6 are not identical, the two figures cannot be superimposed; however, what is important is the general behavior which is very similar. In Fig.7 we exhibit the predicted value of the efficiency parameter γ defined in Eq.(30a,c).

In Fig.8 we exhibit the rate of dissipation of turbulent kinetic energy ϵ vs.depth z with and without the wave breaking phenomenon. As one can observe, the dotted line representing the law of the wall, Eq.(32a), provides a good representation of the data only when the wave breaking phenomenon is not important, which occurs at considerable depths. Near the surface, the data indicate a much larger dissipation rate (crosses and triangles, Terray et al., 1996) which the turbulence model can reproduce quite well (full line) using the dynamic equation for the turbulent kinetic energy (25) with the boundary condition at z=0 given by relation (32b). The values of H_s, u_* and $\bar{c}$ are taken from tables

1,2 of Terray et al.(1996) and from table 1 of Drennan et al.(1996).

XIX. Ocean GCM

To test the new vertical diffusivities, we used the global ocean general circulation model NCAR CSM Ocean Model produced by the University Corporation for Research, National Center for Atmospheric Research, Climate and Global Dynamics Division. They developed the model from the MOM 1.1 GFDL code (see the NCAR CSM Ocean Model Tech. Note, The NCAR CSM Ocean Model, by the NCAR Oceanography section). We employed the stand–alone 3^0x3^0 configuration of the model detailed in their technical note with the default parameter values. It has 3.6^0 spacing in longitude and a variable spacing in latitude increasing from 1.8^0 at the equator to 3.4^0 at 17^0 N, S and then decreasing back to 1.8^0 for 60^0 N, S and poleward. There are 25 levels of increasing thickness in the vertical, with the surface level 6 meters thick. The option for the GM mesoscale eddy parameterization was enabled. Bulk forcing with a seasonal cycle plus a 1/2 year timescale restoring condition on the salinity is used, except under sea–ice where there is strong restoring. This configuration corresponds to the case B–K described in Large et al. (1997). It should be noted, however, that for determination of the length scale in our turbulence model we used the program's definition for mixed layer depth (a buoyancy difference from the surface of 3 $10^{-4}ms^{-2}$), which is different from that graphed as a diagnostic in Fig.5 of Large et al.(1997). We initialized our runs with annually averaged Levitus data and ran for 126 momentum years. As in Large et al. (1997) a 3504sec timestep for momentum is used, while for the first 96 momentum years the tracers are accelerated by a factor increasing from 10 at the surface to 100 for the deep ocean. We then set all timesteps equal for the remaining 30 years as they did.

First, we ran the NCAR program as is, with the option for the KPP mixing enabled, producing the KPP data presented in the figures below. Then, in place of the KPP module, we inserted a module which uses our new model for the diffusivities for momentum and

heat with the salt diffusivity set equal to that of heat. To save computing time, we constructed tables of the dimensionless functions $S_{m,h}$ and of the dimensionless variable y obtained from solving Eq.26a and using Eq.(25c),

$$y \equiv \tfrac{1}{2}x^2(\frac{\ell}{\Lambda})^2 = \tfrac{1}{2}\frac{\Sigma^2\ell^2}{K}, \qquad x^2 \equiv \Lambda^2\Sigma^2K^{-1} \tag{37a}$$

vs. Ri. Then, for each point in space and time these were interpolated to the local Ri. The diffusivities $K_{m,h}$(model) were rewritten as

$$K_{m,h}/\ell^2\Sigma = \tfrac{1}{2}B_1y^{-\frac{1}{2}}S_{m,h} \tag{37c}$$

XX. Below the Mixed Layer

Below the ocean mixed layer, we employed the same background diffusivities as in the NCAR model, specifically:

$$K_m=16.7\ cm^2s^{-1}, \qquad K_h=K_s=0.5\ cm^2s^{-1} \tag{38}$$

XXI. Ocean GCM

The results using the new vertical diffusivities K_m and $K_s=K_h$ are presented in Figs.9–20 where we exhibit the model results (squares) Levitus data (–) and the results using the KPP model (diamonds). We present both global T and S, Figs.9–10, as well as specific basins, artic, atlantic, pacific, indian and southern oceans.

XXII. Conclusions

The goal of this paper was not only that of devising a model for the vertical diffusivities that performs better than previous models. The overall goal had a much wider breadth, that of building a model that satisfies several conditions:

1) the model is not tailored specifically to ocean turbulence like previous model (e.g.,KPP),

2) before being used in an O–GCM, it must be shown to reproduce well documented laboratory, atmospheric and LES data on stratified turbulence, e.g., Figs.3–4, 5–6,

3) it must incorporate the latest advances in turbulent closure modeling so as to naturally give rise to a critical Richardson number (Fig.2) that corresponds not only to the empirical data from mixed layer studies (e.g., Martin, 1985) but which also reproduces laboratory data (e.g., Monin and Yaglom, 1971),

4) in the non–local case, where the flux of turbulent kinetic energy is included in the equation for the kinetic energy, the model must be able to reproduce the observed increase of dissipation caused by breaking waves at the ocean surface, Fig.8,

5) the model not only reproduces the $K_h = \gamma \epsilon N^{-2}$ representation of the heat diffusivity that has been widely used in the past but it predicts a value for γ that varies with Ri, as indeed expected, Fig.7.

6) after these tests have been passed, the model is tested in an O–GCM without changing any of the ingredients that have been used to reproduce 1)–5) above. The model is expected to perform at least as well as previous ad hoc models like KPP. Even in the simplest case, corresponding to a local model, the results shown in Figs.9–20 satisfy this criterion,

7) the strength of the model is its ability to encompass other cases within the same methodology. In the next paper, the model will be extended to include the salinity field thus allowing K_s to be different than K_h, as dictated by laboratory and ocean data.

Appendix A

Pressure Correlation terms

For the tensor Π_{ij}, we employ the most general expression (Canuto 1994):

$$\Pi_{ij} = 2\tau_{pv}^{-1} b_{ij} + (1-\beta_5) B_{ij} - \tfrac{4}{5} K S_{ij} - \alpha_1 \Sigma_{ij} - \alpha_2 Z_{ij} \tag{A.1}$$

where we have defined the following traceless tensors and vectors:

$$b_{ij} = \tau_{ij} - \frac{2}{3} K \delta_{ij}, \qquad h_i = \overline{u_i \theta} \tag{A.2}$$

$$B_{ij} = \lambda_i h_j + \lambda_j h_i - \frac{2}{3} \delta_{ij} \lambda_k h_k \tag{A.3}$$

$$\Sigma_{ij} \equiv S_{ik} b_{kj} + S_{jk} b_{ik} - \frac{2}{3} \delta_{ij} S_{k\ell} b_{k\ell} \tag{A.4}$$

$$Z_{ij} \equiv b_{ik} V_{jk} + b_{kj} V_{ik} \tag{A.5}$$

$$S_{ij} = \tfrac{1}{2}(U_{i,j} + U_{j,i}), \quad V_{ij} = \tfrac{1}{2}(U_{i,j} - U_{j,i}) \tag{A.6}$$

In all the above equations, $\lambda_i = \alpha_T g_i$ ($g_i = 0,0,g$), $\alpha_T = -\rho^{-1} \partial\rho / \partial T$. Analogously, we have (Canuto, 1994)

$$\Pi_i = \tau_{p\theta}^{-1} \overline{u_i \theta} + \gamma_1 \lambda_i \overline{\theta^2} - \tfrac{3}{4} \alpha_3 (S_{ij} + \tfrac{5}{3} V_{ij}) \overline{u_j \theta} \tag{A.7}$$

Appendix B

Third–order moments, TOM

The equations for the third–order moments are taken from Canuto (1994). In the presence of buoyancy, shear and rotation, they are:

$$\left(\frac{D}{Dt} + \tau_3^{-1}\right) \overline{u_i u_j u_k} = -(\overline{u_i u_j u_\ell} U_{k,\ell} + \text{perm}) - (\overline{u_i u_\ell} \frac{\partial}{\partial x_\ell} \overline{u_j u_k} + \text{perm}) + (1 - c_{11})(\lambda_i \overline{\theta u_j u_k} + \text{perm}) - \frac{2}{3\tau}(\delta_{ij} \overline{q^2 u_k} + \text{perm}) \tag{B.1}$$

$$\left(\frac{D}{Dt} + \tau_3^{-1}\right) \overline{u_i u_j \theta} = \overline{u_i u_j u_k} \beta_k - (\overline{u_i u_k} \theta U_{j,k} + \overline{u_j u_k} \theta U_{i,k}) - (\overline{u_i u_k} \frac{\partial}{\partial x_k} \overline{\theta u_j} + \overline{u_j u_k} \frac{\partial}{\partial x_k} \overline{\theta u_i} + \overline{\theta u_k} \frac{\partial}{\partial x_k} \overline{u_i u_j}) +$$

$$\frac{2}{3}c_{11}\delta_{ij}\lambda_k\overline{\theta^2 u_k} + (1-c_{11})(\lambda_i\overline{\theta^2 u_j}+\lambda_j\overline{\theta^2 u_i}) \tag{B.2}$$

$$(\frac{D}{Dt}+\tau_3^{-1}+2\tau_\theta^{-1})\overline{u_i\theta^2} = 2\overline{\theta u_i u_j}\beta_j - \overline{\theta^2 u_j}U_{i,j} - 2\overline{\theta u_j}\frac{\partial}{\partial x_j}\overline{\theta u_i} +$$

$$+ (1-c_{11})\lambda_i\overline{\theta^3} - \overline{u_i u_j}\frac{\partial}{\partial x_j}\overline{\theta^2} \tag{B.3}$$

$$(\frac{D}{Dt} + \frac{c_{10}}{c_*}\tau_3^{-1})\overline{\theta^3} = 3\beta_j\overline{\theta^2 u_j} - 3\overline{\theta u_j}\frac{\partial}{\partial x_j}\overline{\theta^2} + \chi\frac{\partial^2}{\partial x_\ell^2}\overline{\theta^3} \tag{B.4}$$

where $\tau_3 \equiv \tau/2c_*$ and $c_*=7$, $c_{10}=4$, $c_{11}=1/5$. In the absence of shear, and in the stationary case, Eqs. (B.1)–(B.4) were solved analytically. The resulting third–order moments exhibited some unexpected symmetry properties in that they they are all given by the sum of the gradients of all the second–order moments, see Eq.(5d). These new expressions for the TOM were shown to reproduce quite well the LES data for a buoyancy driven PBL (Canuto et al., 1994).

Appendix C

Wave breaking case. Boundary condition for K

Craig and Banner (1994) first suggested that at z=0 one takes the flux of turbulent kinetic energy F(K), see Eq.(7c), equal to

$$F(K,z=0) = \alpha u_*^3, \quad \alpha\sim 10^2 \tag{C.1}$$

where u_* is the wind stress at the surface. To translate (C.1) into a relation for the kinetic energy at z=0, we proceed in a different manner than Craig and Banner. Consider the stationary limit of Eq.(25) near the surface. In the absence of a heat flux, we obtain

$$K_m S^2 + \frac{\partial}{\partial z}(K_m\frac{\partial K}{\partial z}) = \epsilon \tag{C.2}$$

Since $N^2\sim 0$, Eq.(20a) for K_m becomes $K_m = c_1 K^2\epsilon^{-1}$, $c_1 \equiv 2S_m$=constant and (C.2) becomes

$$K_m^2 S^2 + K_m\frac{\partial}{\partial z}(K_m\frac{\partial K}{\partial z}) = c_1 K^2 \tag{C.3}$$

Since near the surfacer $K_m S^2 \equiv -\overline{uw}S_{13} = u_*^2$ and since $K^2 >> u_*^2$, Eq.(C.3) becomes

$$\frac{\partial^2 K}{\partial \xi^2} = K^2, \qquad c_1^{-\frac{1}{2}} K_m \frac{\partial}{\partial z} = \frac{\partial}{\partial \xi} \tag{C.4}$$

Multiplying both sides of (C.4) by $\partial K/\partial \xi$, we obtain

$$\frac{\partial}{\partial \xi}\left(\frac{\partial K}{\partial \xi}\right)^2 = \frac{2}{3}\frac{\partial K^3}{\partial \xi} \tag{C.5}$$

which can be integrated to yield

$$K_m \frac{\partial K}{\partial z} = AK^{3/2}, \qquad A^2 \equiv \frac{2}{3}c_1 \tag{C.6}$$

Using the second of (C.1), we obtain

$$\alpha u_*^3 = AK^{3/2} \tag{C.7}$$

Since (Terray et al, 1996, Eq.5)

$$\alpha = \bar{c}/u_* \tag{C.8}$$

and using $K=\frac{1}{2}q^2$, we finally obtain that at z=0 the velocity q is given by:

$$q = (12c_1^{-1})^{1/6}\, u_*^{2/3}\, \bar{c}^{1/3} \tag{C.9}$$

which is relation (32b) of the text.

Appendix D

Alternative Determination of the constants (14d)

To determine the constants appearing in Eqs.(14e–f), we adopt from Shih and Shabbir (1992) and Canuto (1993) the expressions

$$\begin{aligned} \lambda_2 &= (1-\alpha_1)\,(2c_4^*)^{-1}, \quad \lambda_3 = (1-\alpha_2)(2c_4^*)^{-1} \\ \lambda_4 &= \beta_5 (2c_4^*)^{-1}, \quad \lambda_6 = 1 - \frac{3}{4}\alpha_3 \\ \lambda_7 &= 1 - \frac{5}{4}\alpha_3, \qquad \lambda_8 = (1-\gamma_1)\frac{\tau}{\bar{\tau}}\theta \end{aligned} \tag{D.1}$$

where

$$\begin{aligned} c_4^* &= 2 + 6.22\, F^2(1-F)^{3/4} - F^{\frac{1}{2}} \\ \alpha_1 &= 6\alpha_5, \qquad \alpha_2 = \frac{2}{3}(2 - 7\alpha_5) \\ \alpha_5 &= \frac{1}{10}\left(1 + \frac{4}{5}F^{\frac{1}{2}}\right), \qquad \alpha_3 = \frac{4}{5} \\ F &= 0.64, \quad \beta_5 = 0.48 \end{aligned} \tag{D.2}$$

The values thus obtained are

$$(\lambda_2, \lambda_3, \lambda_4, \lambda_6, \lambda_7) = (0.00336, 0.0906, 0.101, 0.4, 0) \tag{D.3}$$

To determine $\lambda_{1,5}$, we employ a neutral surface layer in which the mean profiles are logarithmic, the mean wind is along the x–direction and z approaches zero,

$$-\overline{uw} = u_*^2, \quad \tau \frac{dU}{dz} = (q/u_*)^2, \quad \tfrac{1}{2}q^2 \equiv K \tag{D.4}$$

Under these conditions, the algebraic equations for $\overline{u}^2$, $\overline{v}^2$ and $\overline{w}^2$, Eqs.(18a–c), can be simplified and yield

$$\lambda_1 = \frac{4}{3}(3\lambda_3^2 - \lambda_2^2) + 4B_1^{-4/3} \tag{D.5}$$

where

$$B_1 \equiv (q/u_*)^3 = 16.6 \tag{D.6}$$

in accord with the MY model. Using the values of λ_2 and λ_3 given in (D.3), we obtain

$$\lambda_1 = 0.127 \tag{D.7}$$

The value of λ_5 is obtained in a similar fashion. Assuming that production equals dissipation in the above neutral surface layer, we have

$$Sh = 2B_1^{-4/3}\sigma_{t_0}^{-1}, \quad \sigma_{t_0} = 1 \tag{D.8}$$

where σ_{t_0} is the turbulent Prandtl number in the neutral case which we take to be unity. Applying the neutral condition and $z \to 0$ to the equations for $\overline{u\theta}$, $\overline{w\theta}$, Eqs.(19a,b), and using

$$\overline{w\theta} = -K\tau S_h \frac{dT}{dz} \tag{D.9}$$

after some algebra we get an algebraic equation for λ_5,

$$\lambda_5^2 - \frac{1}{3}B_1^{4/3}(1 + \lambda_2 - 3\lambda_3)\sigma_{t_0}\lambda_5 - \frac{1}{4}(\lambda_6 - \lambda_7)B_1^{4/3}(\lambda_6 + \lambda_7 + 2\sigma_{t_0}) = 0 \tag{D.10}$$

The solution is

$$\lambda_5 = 11.2 \tag{D.11}$$

Similarly, from the algebraic equation for $\overline{\theta}^2$, Eq.(8a), we have

$$\frac{\tau_\theta}{\tau} = \sigma_{t_0}^{-1} B_1^{-2/3} Q, \quad Q \equiv \overline{\theta}^2 u_*^2 / (\overline{w\theta})_s^2 = 3.1 \tag{D.12}$$

where the subscript s indicates a surface quantity, and Q=3.1 in accordance with Mellor and Yamada (1982). Substituting (D.12) into (D.1) and using γ_1=1/3 gives

$$\lambda_8 = (1 - \gamma_1)\frac{\tau_\theta}{\tau} = 0.318 \tag{D.13}$$

Figure caption

Fig.1. Model predictions for the dimensionless structure functions S_m and S_h defined in Eq.(20a) vs. the degree of stability Ri.

Fig.2. The time scale τ, specifically, the variable ψ, Eq.(26c), vs. the degree of stability Ri, see Eq. (26c). Since Eq.(27) shows that ψ is the inverse of the turbulent kinetic energy K, this figure shows that at $Ri_{cr}\sim 1$, K vanishes for the stratification is to strong for turbulent mixing to survive. Several 1–point closure models of the Mellor–Yamada type predict a far smaller $Ri_{cr}\tilde{}0.25$ which considerably reduces the extent of turbulent mixing

Fig.3. Laboratory data for the turbulent Prandtl number σ_T vs.Ri (Webster 1964); σ_T is defined in Eq.(20b) and is the ratio of S_m/S_h presented in Fig.1.

Fig.4. The turbulent Prandtl number $\sigma_T = S_m/S_h$ vs. Ri predicted by the present model. Several previous models predict a constant σ_T.

Fig.5. The predicted flux Richardson number R_f vs. Ri, see Eq.(30c).

Fig.6. The flux Richardson number R_f vs. Ri from a variety of laboratory data. The symbols refer to different authors cited in Maderich et al. (1995) and refer to either grid generated turbulence and/or freely decaying turbulence in a stably stratified medium. Since the Ri used in Figs.5–6 are not identical, a superposition of the two figures in not possible. What is important is that the general behavior predicted by the model mirrors that of the data.

Fig.7. Efficiency parameter γ(Ri) defined in Eq.(30a,c) vs. Ri. Even though a great deal of caution must be exercised in using the data (see discussion after Eq.30c), an observed value of $\gamma\sim 1/4$ (e.g., Oakey, 1982; Toole et al., 1994) is found to correspond to an Ri~0.25 which is well within the expected values.

Fig.8. The rate of dissipation of turbulent kinetic energy $\epsilon(z)$ vs. depth z in meters. The predicted value of $\epsilon(z)$ in the absence of the wave–breaking phenomenon (dashed line) is a poor representation of the data (crosses and diamonds) in the first 10 meters. A much more

realistic prediction (solid line) is achieved if wave–breaking is included in the turbulence model. This requires a non–local model, the details of which are discussed in Appendix C.

Fig.9. When the new expressions for $K_{m,h}$ and $K_s=K_h$ are used in the O–GCM, we obtain the results exhibited in Figs.9–20. To ease the comparison, we also ran the same O–GCM with the KPP model. The model results are compared with Levitus et al. (1994) data. Global temperature vs. depth.

Fig.10. Same as Fig.9 for the global salinity

Fig.11. Same as Fig.9 for the Artic ocean

Fig.12. Same as Fig.10 for the Artic ocean

Fig.13. Same as Fig.9 for the Atlantic ocean

Fig.14. Same as Fig.10 for the Atlantic ocean

Fig.15. Same as Fig.9 for the Pacific ocean

Fig.16. Same as Fig.10 for Pacific ocean

Fig.17. Same as Fig.9 for the Indian ocean

Fig.18. Same as Fig.10 for the Indian ocean

Fig.19. Same as Fig.9 for the Southern ocean

Fig.20. Same as Fig.10 for the Southern ocean

References

Agrawal, Y.C., E.A.Terray, M.A.Donelan, P.A.Hwang, A.J.Williams III, W.M.Drennan, K.K. Kahma and S.A.Kitaigorodskii, 1992: Enhanced dissipation of kinetic energy beneath surface waves. *Nature*, **359**, 219–220

Anis, A. and J.N. Moum, 1994: Prescriptions for the heat flux and entrainment rates in the upper ocean during convection. *J. Phys. Oceanogr.*, **24**, 2142–2155

Baum, E. and E.A.Caponi, 1992: Modeling the effects of buoyancy on the evolution of geophysical boundary layer. *J.Geophys. Res.*, **97,** 15513–15527

Blanke, B. and P. Delecluse, 1993: Variability of the tropical atlantic ocean simulated by the general circulation model with two different mixed layer physics, *J. Phys. Oceanogr.*. **23,** 1363–1388

Burchard, H. and H. Baumert, 1995: On the performance of a mixed–layer model based on the K–ϵ turbulence closure. *J. Geophys. Res.*, **100**, 8523–8540

Burgers, G., 1997: Comments on "Estimates of kinetic energy dissipation under breaking waves". *J. Phys. Oceanogr.*, **27**, 2306–2307

Canuto, V.M., 1994: Large eddy simulation of turbulence: a subgrid model including shear, vorticity, rotation and buoyancy, *ApJ*, **428**, 729–752

Canuto, V.M., F. Minotti, C. Ronchi, M. Ypma and O. Zeman, 1994: Second–order closure PBL model with new third–order moments: comparison with LES data. *J. Atm. Sci.*, **51,** 1605–1618

Cheng, Y. and V.M. Canuto, 1994: Stably stratified turbulence: a new model for the energy dissipation length scale, *J. Atm. Sci.*, **51**, 2384–2396

Chou, P.Y, 1940: On an extension of Reynolds method of finding apparent stresses and the nature of turbulence, *Chinese J. Phys.*, **4**(1), 1–33

Chou, P.Y., 1945: On velocity correlations and the solutions of the equations of the turbulent fluctautions, *Quart. Applied Math.*, **3**(1), 38–54 .

Craig, P.D. and M.L. Banner, 1994: Modeling wave–enhanced turbulence in the ocean

surface layer. *J. Phys. Oceanogr.*, **24**, 2546–2559

Cummings, P.F., G. Holloway and A.E. Gargett, 1990: Sensitivity of the GFDL ocean circulation model to a parameterization of vertical diffusion. *J. Phys. Oceanogr.*, **20**, 817–830

D'Alessio, S.J.D., K. Abdella and N.A. McFarlane, 1998: A new second–order turbulence scheme for modeling the ocean mixed layer. *J.Phys. Oceanogr.*, **28**, 1624–1641

Davis, R.E., 1994: Dyapicnal mixing in the ocean: the Osborn–Cox model. *J. Phys. Oceanogr.*, **24**, 2560–2576

Deardorff, J. W. 1980: Stratocumulus capped mixed layer derived from a three dimensional model. *Bound. Layer Met.* **18**, 495–527

Dewan, E.M., 1979: Stratospheric spectra resembling turbulence, *Science*, **204**, 832–835

Hunt, J. C. R., Stretch, D. D., Britter, R. E., Length scales in stably stratified turbulent flows and their use in turbulence models, in *Stably Stratified Flows and Dense Gas Dispersion* (J. S. Puttock, ed.), pp. 285, Clarendon Press, Oxford, 1988

Drennan, W.M., M.A.Donelan, E.A.Terray, K.B.Katsaros, 1996: Oceanic turbulence dissipation measurements in SWADE. *J. Phys. Oceanogr.*, **26**, 808–815

Fernando, H.J.S. and Hunt, J.C.R., 1996: Some aspects of turbulence and mixing in stably stratified layers, *Dyn. Atm. and Oceans*, **23**, 35–62

Galperin, B., A.Rosati, L.H. Khanta and G.L. Mellor, 1989: Modeling rotating stratified turbulent flows witha pplication to oceanic mixed layer. *J. Phys. Oceanogr.*, **19**, 901–916

Gargett, A. E., P. J. Hendricks, T. B. Sanford, T. R. Osborn and A. J. Williams 1981: A composite spectrum of vertical shear in the upper ocean. *J. Phys. Oceanogr.* **11**, 1258–1271

Gargett, A. E. 1984: Vertical eddy diffusivity in the ocean interior. *J. Mar. Res.* , **42**, 359–393

Gargett, A. E. 1989: Ocean turbulence. *Ann. Rev. Fluid Mech.*, **21**, 419–451

Gaspar, P., Y. Gregoris, and J.M. Lefevre, 1990: A simple eddy kinetic energy model for simulations of the oceanic vertical mixing: test at station Papua and long–term upper ocean study site. *J.Geophys. Res.*, **95,** 16179–16193

Gatski, T.B., Sarkar, S. and Speziale, C.G, Eds. *Studies in Turbulence*, Spinger–Verlag, New York, pp. 602

Holland, W.R., 1989: Experience with various parameterizations of sub–grid scale dissipation and diffusion in numerical models of ocean circulation, in *Parameterization of small scale processes*, Proc. Hawaiian Winter Workshop, Univ. Hawaii, Jan. 17–20, 1–11

Hunt, J.R.C., D.D. Strecht and R.E. Britter, 1988: Length scales in stably stratified turbulence flows and their use in turbulence models, in *Stably Stratified Flows and Dense Gas Dispersion,* J.S. Puttock, Ed. Clarendon Press, 285–321

Khanta, L. and C.A. Clayson, 1994: An improved mixed layer model for geophysical applications. *J. Geophys. Res.*, **99**, C12, 25235–25266

Kitaigorodskii, S.A., M.A.Donelan, J.L Lumley and E.A. Terray, 1983: Wave–turbulence interactions in the upper ocean, part II. *J. Phys. Oceanogr.*, **13,** 1988–1999

Kraichnan, R. H, 1964: Decay of isotropic turbulence in the Direct Interaction Approximation, *Phys. Fluids*, **7**, 1030–1042

Large, W.G., J.C. McWilliams, and S.C. Doney, 1994: Oceanic vertical mixing: a review and a model with non–local boundary layer parameterization. *Rev. of Geophys.*, **32**, 4, 363–403

Launder, B. E., G. J. Reece and W. Rodi, 1975: Progress in the development of a Reynolds stress turbulent closure. *J. Fluid Mech.*, **68**, 537–566

Leslie, D.C., 1973: *Developments in the the theory of turbulence*, Clarendon Press, Oxford. pp 368

Levitus, S., R.Burgett and T.P. Boyer, 1994: *World Ocean Atlas 1994, Vol.3: Salinity,* NOAA Atlas NESDIS 3, 111 pp.

Levitus, S., and T.P. Boyer, 1994: *World Ocean Atlas 1994, Vol.4: Temperature* , NOAA Atlas NESDIS 4, 129pp

Lumley, J. L., 1964: The spectrum of nearly inertial turbulence in a stably stratified fluid. *J. Atm. Sci.*, **21**, 99–102

Lumley, J.L. and B. Khajeh–Nouri, 1974: Computational modeling of turbulent transport. *Adv. in Geophys.*, **18A**, 169–192

Lumley, J. L. 1978: Computational modeling of turbulent flows. *Adv. in Applied Mech.* 18, 123–176

Ma, C.C., C.R. Mechoso, A. Arakawa and J.D. Ferrara, 1994: Sensitivity of a coupled ocean–atmosphere model to physical parameterizations. *J. Phys. Oceanogr.*, 7, 1883–1896

Maderich, V.S., O.M. Konovalov and S.I. Konstantinov, 1995: Mixing efficiency and processes of restratification in a stably stratified mendium, in *Mixng in Geophysical Flows*, Eds. J.M. Redondo and O. Metais, Int.Center for Num. Methods in Engin., CIMNE, Barcelona, 393–401.

Martin, P. J., 1985, Simulation of the Mixed Layer at OWS November and Papa with several models. *J. Geophys. Res.*, **90**, C1, 903–916

Matear, R.J. and C.S. Wong, 1997: Estimation of vertical mixing in the upper ocean at Station P from chlorofluorocarbons. *J. Marine Res.*, **55**, 507–521

Malsowe, S.A., in *Hydrodynamic Instabilities and the Transition to Turbulence*, Eds. Swinney, H.L and Gollup, J.P., Springer–Verlag, New York, 1981, p.181

McWilliams, J.C. 1996: Modeling the ocean general circulation. *Ann. Rev. Fluid Mech.*, **28**, 215–248

Mellor, G.L. 1989: Retrospect on oceanic boundary layer modeling and second moment closure, in *Parameterization of small scale processes*, Proc. Hawaiian Winter Worshop, Univ. Hawaii, Jan. 17–20, 251–272

Mellor, G. L. and T.Yamada, 1982: Development of a turbulence closure model for

geophysical fluid problems. *Rev. of Geophys. and Space Phys.* **20,** 85–875

Moeng, C–H. and J.C. Wyngaard, 1989: Evaluation of turbulent transport and dissipation closures in second–order modeling, *J. Atmos. Sci.*, **46**, 2311–2330

Monin A. S. and A. M. Yaglom, 1971: *Statistical Fluid Mechanics,* Vol. 1, 2, MIT Press

Moum, A.S., 1989: Measuring turbulent fluxes in the Ocean. The quest for K_ρ. in *Parameterization of small scale processes*, Proc. Hawaiian Winter Worshop, Univ. Hawaii, Jan. 17–20, 145–156

Oakey, N.S., 1982: Determination of the rate of dissipation of turbulent energy from simultaneous temperature and velocity shear microstructure measurements. *J. Phys. Oceanogr.*, **12**, 256–271

Osborne, T.R., 1980: Estimates of the local rate of vertical diffusion from dissipation measurements. *J. Phys. Oceanogr.*, **10**, 83–89

Polzin, K.L, J.M. Toole,, J.R. Ledwell, and R.W. Schmitt, 1997: Spatial variability of turbulent mixing in abyssal ocean. *Science,* **276**, 93–96

Pope. S. B., 1975: A more general effective viscosity hypothesis. *J. Fluid Mech.*, **72**, 331–340.

Rodi, W., 1984: *Turbulence Models and their Application*, IAHR, Rotterdamseweg 185, P.O. Box 177, Delft, The Netherlands, 104 p.

Rosati. A. and K. Miyakoda, 1988: A general circulation model for upper ocean simulation. *J. Phys. Oceanogr.* **18**, 1601–1626

Shih, T. S. and A. Shabbir, 1992: Advances in modeling the pressure correlation terms in the second moment equations, in *Studies in Turbulence*, Eds. T. B. Gatski, S. Sarkar, and C. G. Speziale, 91–128, Springer–Verlag

Skyllingstad, E.D., W.D. Smyth, J.N. Moum, and H.Wijesekera, 1999: Upper–Ocean Turbulence during a Westerly Wind Burst: A comparison of Large–Eddy Simulation Results and Microstructure Measurements. *J. Phys. Oceanogr.*, **29**, 5–28

Terray, E.A., M.A.Donelan, Y.C. Agrawal, W.M.Drennan, K.K. Kahma, A.J. Williams

III, P.A. Hwang, and S.A. Kitaigorodskii, 1996, Estimates of kinetic energy dissipation under breaking waves. *J. Phys. Oceanogr.*, **26**, 792–807

Terray, E.A., M.A.Donelan, Y.C. Agrawal, W.M.Drennan, K.K. Kahma, A.J. Williams III, P.A. Hwang, and S.A. Kitaigorodskii, 1997, Reply. *J. Phys. Oceanogr.*, **27**, 2308–2309

Thorpe, S.A., 1977: Turbulence and mixing in a scottish loch. *Phil. Trans. Roy.Soc. London, Ser.A,* **286**, 125–181

Toole, J. M., K. L. Polzin and R. W. Schmitt, 1994: Estimates of diapycnal mixing in the abyssal ocean. *Science*, **264**, 1120–1123

Wang, D. W.G. Large and J.C.McWillimas, 1996: Large Eddy simualtion of equatorial boundary layer: diurnal cycle, eddy viscosity and horizotal rotation. *J. Geophys. Res.* **101**, 3649–3662

Webster, C. A. G. 1964: An experimental study of turbulence in a density stratified shear flow. *J. Fluid Mech.*, **19**, 221–245

Weinstock, J. 1978: On the theory of turbulence in the buoyancy subrange of stably stratified flows. *J. Atm. Sci.*. **35**, 634–64

Weinstock, J., 1981: Energy dissipation rates of turbulence in the stable free atmosphere. *J. Atmos. Sci.*, **38**, 880–

Wuest, A., D.C. van Senden, J.Imberger, G.Piepke and M.Gloor, 1996: Comnparison of diapycnal diffusivity measured by tracer and microstucture techniques, Dyn. Atmos. and Oceans, **24**, 27–39

Rodi, W., *Turbulence Models and their Application*, IAHR, Rotterdamseweg 185, P.O. Box 177, Delft, The Netherlands, 104 p.

Sarmiento, J. L., H. W. Feely, W. S. Moore, A. E. Bainbridge and W.S. Broeker, 1976: The relationship between vertical eddy diffusivity and buoyancy gradient in the deep sea, *Earth Planet. Sci. Lett.*, 32, 357–370

XIV. Passive Scalar

In Appendix C we develop a model to compute the diffusivity K_c for a passive scalar, e.g., tritium. The mean concentration C satisfies the equation

$$\frac{DC}{Dt} = -\frac{\partial}{\partial x_i}\overline{u_i c} \tag{30a}$$

Here, $\overline{u_i c}$ is the turbulence–induced concentration flux. In the stationary, local case,

$$\overline{wc} = -K_c\frac{\partial C}{\partial z} \tag{30b}$$

where the passive scalar diffusivity K_c is given by:

$$K_c = A^{-1}\tau_{pc}[\overline{w^2} + (1-\gamma_1)\tau_{c\theta}g\alpha_T\,\overline{w\theta}] \tag{30c}$$

with

$$A \equiv 1 + (1-\gamma_1)\tau_{pc}\tau_{c\theta}N^2 \tag{30d}$$

Using Eqs.(18c) and (19a) for the turbulent variables $\overline{w^2}$ and $\overline{w\theta}$, we can express (30c) in the same functional form as (20a,b), namely

$$K_c = 2S_c\frac{K^2}{\epsilon}, \qquad S_c = \frac{2}{3A}\frac{\tau_{pc}}{\tau}(1 - \tfrac{1}{2}\psi\Delta) \tag{30e}$$

with $\Delta>0$ given by:

$$\Delta = \Delta_0 S_m + \Delta_1 S_h Ri \tag{30g}$$

$$\Delta_0 = 3\lambda_3 - \lambda_2, \quad \Delta_1 = 4\lambda_4 + 3(1-\gamma_1)\tau_{c\theta}\tau^{-1} \tag{30h}$$

$$A = 1 + (1-\gamma_1)\tau_{pc}\tau_{c\theta}\tau^{-2}\psi Ri \tag{30i}$$

We recall that ψ is given by Eqs.(28c–e). As for the time scales, we suggest to identify $\tau_{pc}=\tau_{p\theta}$, $\tau_{\theta c}=\tau_\theta$ and employ (4f–g).

The case of a passive scalar

Following the formalism developed in Canuto (1994), the dynamic equation for the turbulent velocity u_i is given by:

$$\frac{Du_i}{Dt} = -u_j U_{i,j} - \frac{\partial p}{\partial x_i} - \frac{\partial}{\partial x_j}(u_i u_j - \overline{u_i u_j}) + \lambda_i \theta + \nu \frac{\partial^2 u_i}{\partial x_j^2} \tag{C.1}$$

while that of the fluctuating temperature θ is:

$$\frac{D\theta}{Dt} = -u_i T_{,i} - \frac{\partial}{\partial x_i}(u_i \theta - \overline{u_i \theta}) + \chi_T \frac{\partial^2 \theta}{\partial x_j^2} \tag{C.2}$$

If we further consider a passive scalar field C, the corresponding turbulent component c satisfies the equation:

$$\frac{Dc}{Dt} = -u_i C_{,i} - \frac{\partial}{\partial x_i}(u_i c - \overline{u_i c}) + \chi_c \frac{\partial^2 c}{\partial x_j^2} \tag{C.3}$$

where χ_c is the kinematic diffusivity of the c–field. To construct the required correlation $\overline{wc}$. we multiply (C.1) by c, (C.3) by u_i, average the results and sum the results. We obtain:

$$\frac{D}{Dt}\overline{cu_i} + D_f = -(\overline{u_i u_j} C_{,j} + \overline{cu_j} U_{i,j}) + \lambda_i \overline{\theta c} - \Pi_i^c - \epsilon_c^i \tag{C.4}$$

where

$$D_f = \frac{\partial}{\partial x_j}(\overline{cu_i u_j}), \qquad \Pi_i^c \equiv <c\frac{\partial p}{\partial x_i}>, \quad \epsilon_c^i \equiv \nu \overline{cu_{i,jj}} \tag{C.5}$$

where we have used <..> instead of a bar for notational convenience and where ϵ_c^i represents the dissipation of $\overline{cu_i}$ due to molecular forces. For Π_i^c we employ an expression analogous to (A.7) but retain only the first two terms,

$$\Pi_i^c = \tau_{pc}^{-1} \overline{u_i c} + \gamma_1 \lambda_i \overline{c\theta} \tag{C.6}$$

Clearly, we need the correlation $\overline{\theta c}$, which we derive using Eqs.(C.2)–(C.3). The result is:

$$\frac{D}{Dt}\overline{c\theta} + D_f = -(\overline{u_i \theta}\frac{\partial C}{\partial x_j} + \overline{u_j c}\frac{\partial T}{\partial x_j}) + \chi_T \overline{c\theta}_{,jj} + \chi_c \overline{\theta c}_{,jj} \tag{C.7}$$

The last two terms can be rearranged to read

$$\chi_T \overline{c\theta}_{,jj} + \chi_c \overline{\theta c}_{,jj} = \tfrac{1}{2}(\chi_c + \chi_T)(\overline{\theta c})_{,jj} - (\chi_c + \chi_T)\,\overline{\theta_{,j} c}_{,j} + \tfrac{1}{2}(\chi_c - \chi_T)[(\overline{\theta c}_{,j})_{,j} - (\overline{c\theta}_{,j})_{,j}] \tag{C.8}$$

The first term may be incorporated with the diffusion term, the last term can be neglected

compared with others while the second term, taking into account that $\chi_T >> \chi_S$, can be parameterized as

$$(\chi_c+\chi_T)\,\overline{\theta_{,j}\sigma_{,j}} = \tau_{c\theta}^{-1}\,\overline{\theta c} \tag{C.9}$$

so that finally

$$\frac{D}{Dt}\overline{c\theta} + D_f = -\left(\overline{u_i\theta}\,\frac{\partial C}{\partial x_j} + \overline{u_j c}\,\frac{\partial T}{\partial x_j}\right) - \tau_{c\theta}^{-1}\,\overline{\theta c} \tag{C.10}$$

In the stationary, local (no diffusion) case, the model gives:

$$\tau_{c\theta}^{-1}\,\overline{\theta c} = -\left(\overline{u_i\theta}\,\frac{\partial C}{\partial x_i} + \overline{u_i c}\,\frac{\partial T}{\partial x_i}\right) \tag{C.11}$$

$$\tau_{pc}^{-1}\,\overline{u_i c} = -\left(\overline{u_i u_j} C_{,j} + \overline{cu_j} U_{i,j}\right) + \lambda_i(1-\gamma_1)\overline{\theta c} \tag{C.12}$$

Thus,

$$A_{ij}\overline{u_j c} = -(K_c)_{ij}\,\frac{\partial C}{\partial x_j} \tag{C.13}$$

where

$$A_{ij} \equiv \delta_{ij} + \tau_{pc}\left[U_{i,j} + (1-\gamma_1)\lambda_i\tau_{c\theta}T_{,j}\right] \tag{C.14}$$

$$(K_c)_{ij} \equiv \tau_{pc}\left[\overline{u_i u_j} + (1-\gamma_1)\tau_{c\theta}\lambda_i\,\overline{u_j\theta}\right] \tag{C.15}$$

In the case of vertical diffusivities, we further have

$$\overline{wc} = -K_c\frac{\partial C}{\partial z} \tag{C.16}$$

where the passive scalar diffusivity K_c is given by:

$$K_c = A^{-1}\tau_{pc}\left[\overline{w^2} + (1-\gamma_1)\tau_{c\theta}g\alpha_T\,\overline{w\theta}\right] \tag{C.17}$$

with

$$A \equiv 1 + (1-\gamma_1)\tau_{pc}\tau_c N^2 \tag{C.18}$$

We recall that $\overline{w^2}$ and $\overline{w\theta}$ are provided by the turbulence model.

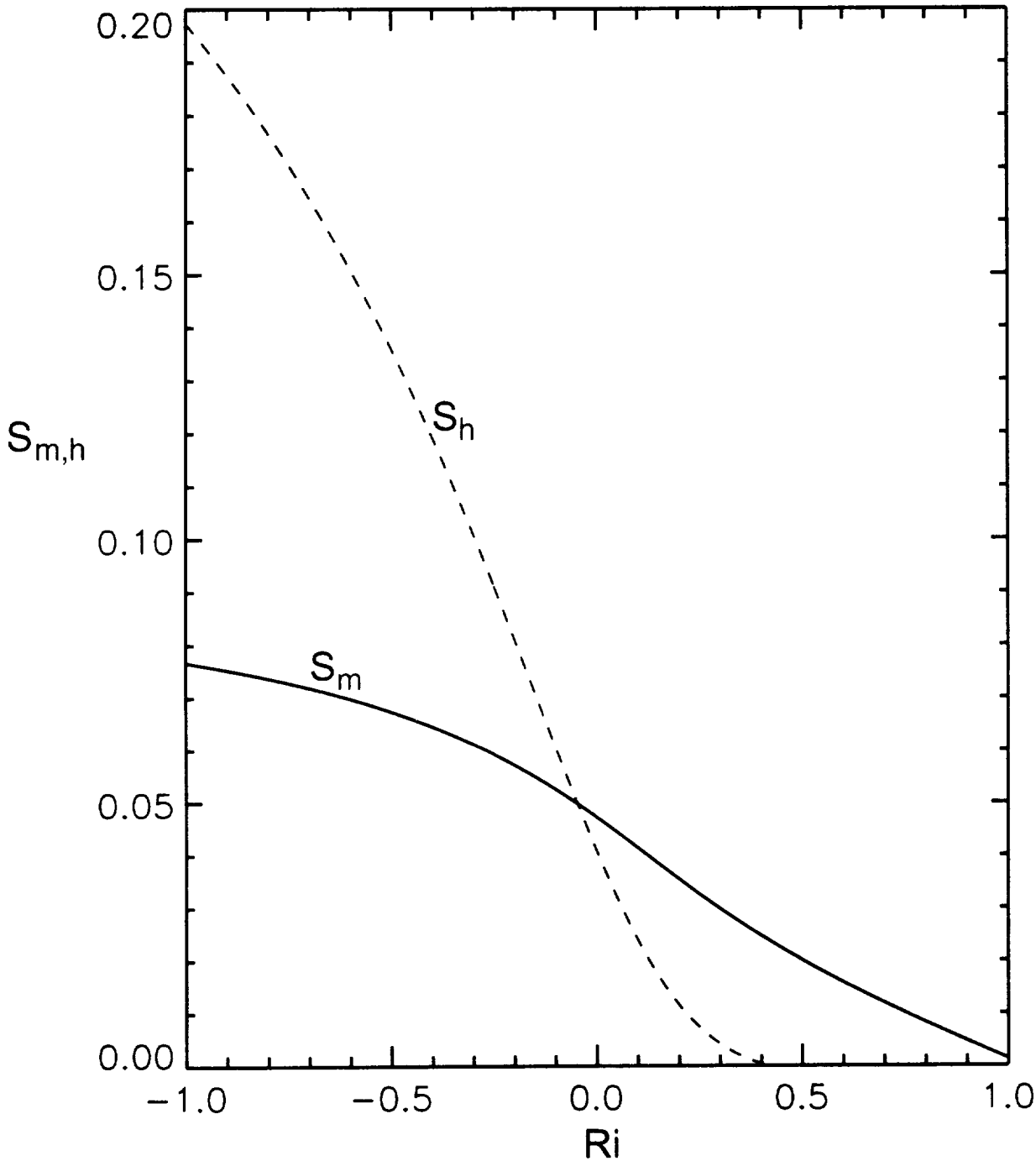

Fig. 1

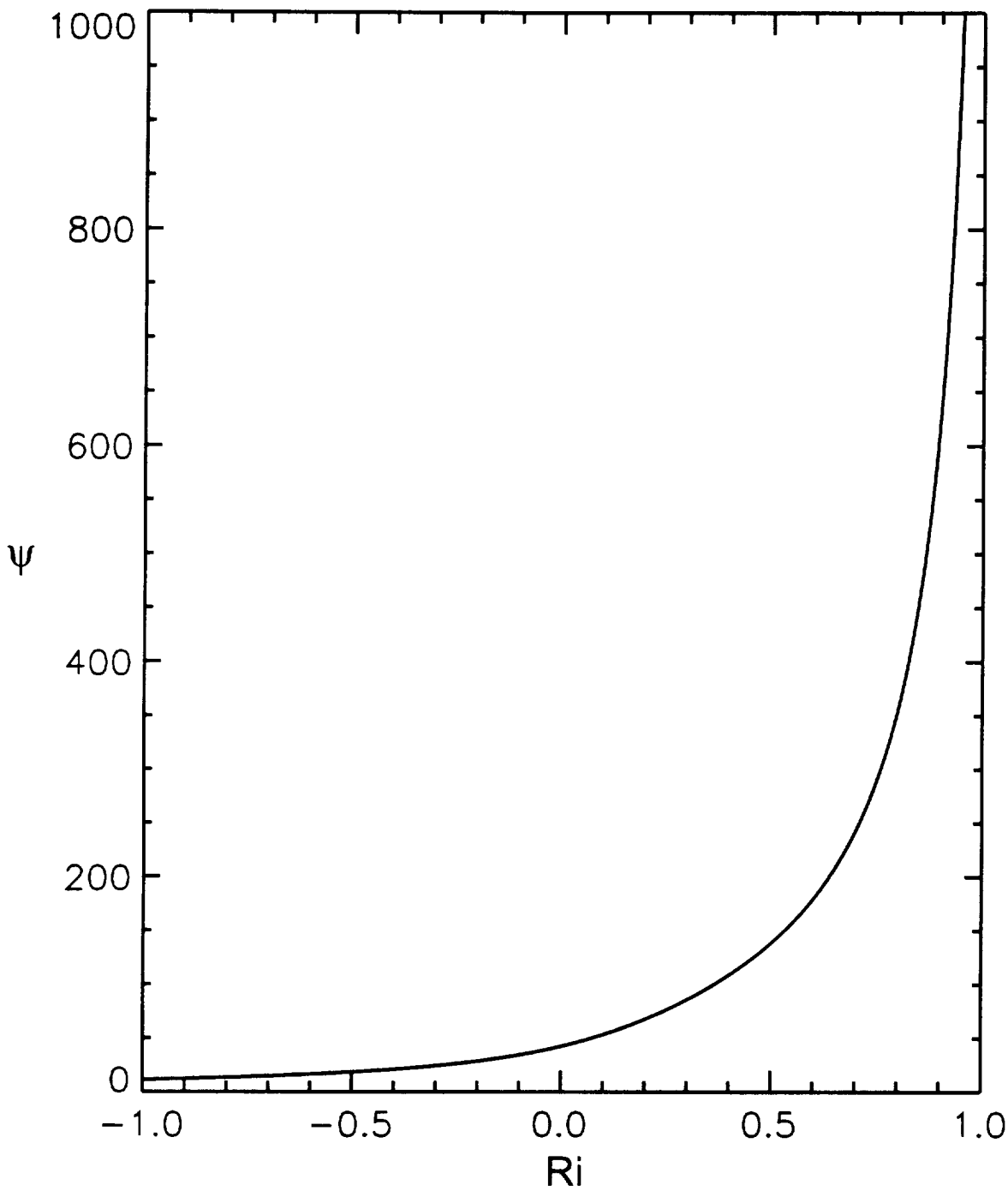

Fig. 2

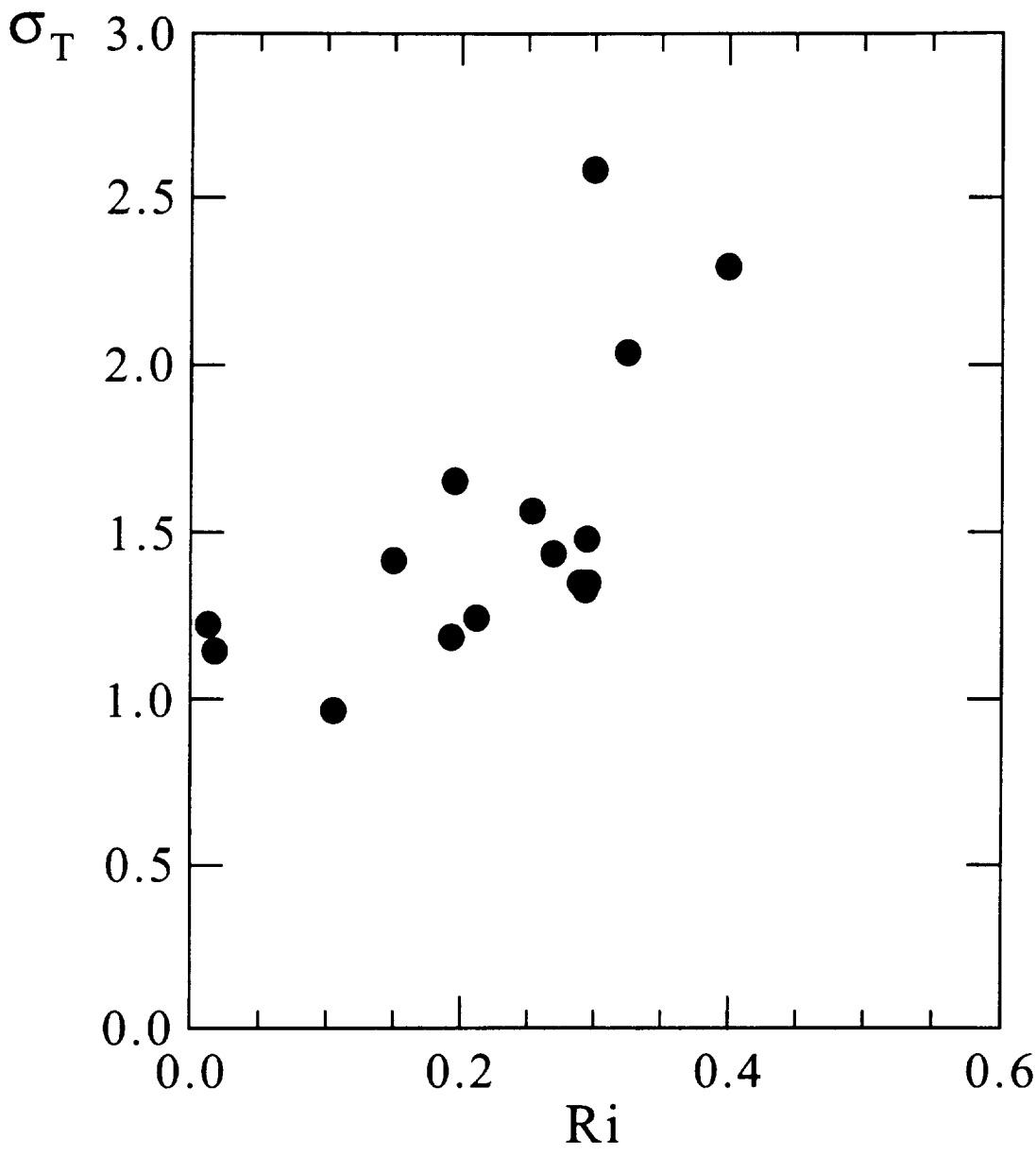

Fig. 3

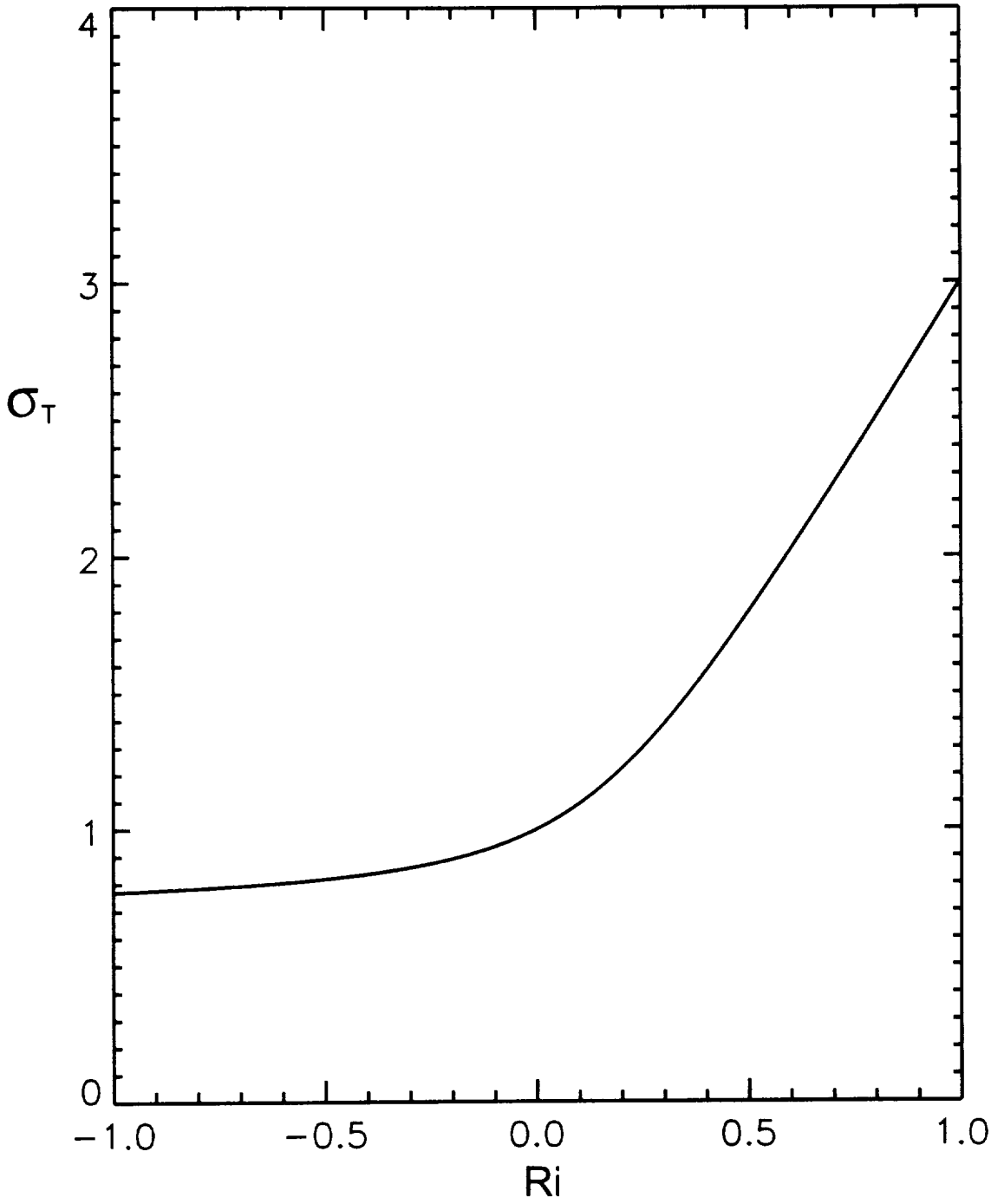

Fig. 4

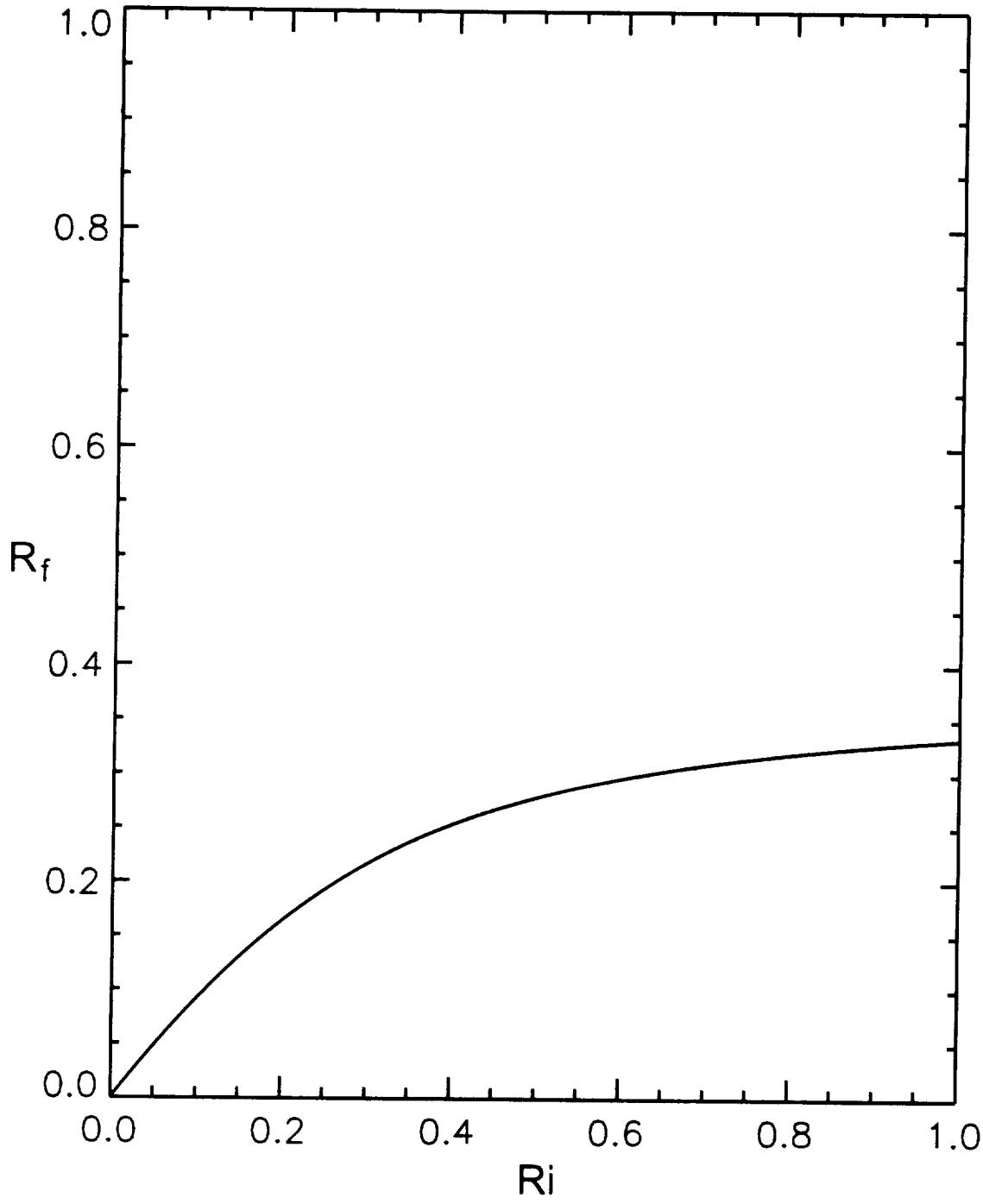

Fig. 5

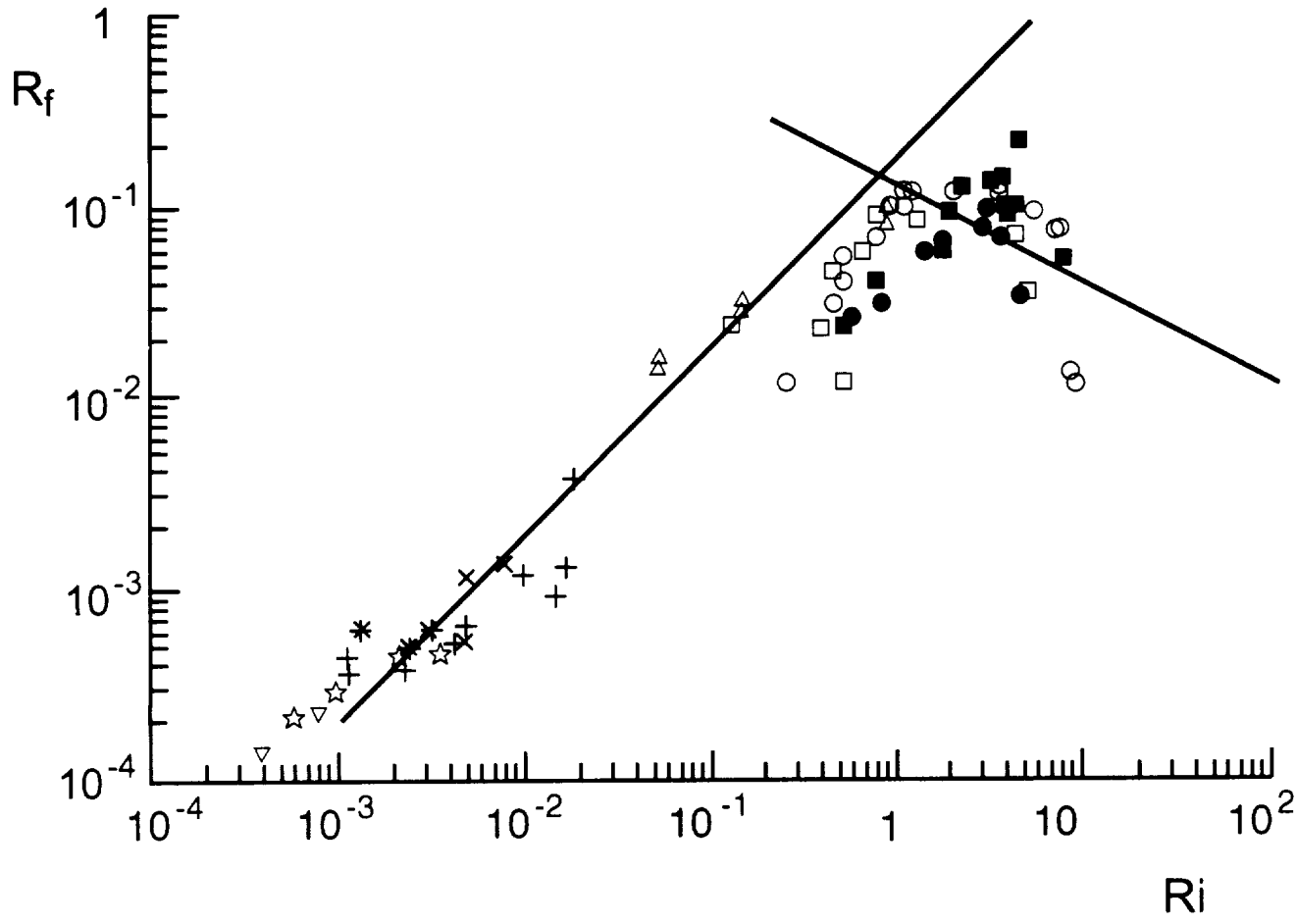

Fig. 6

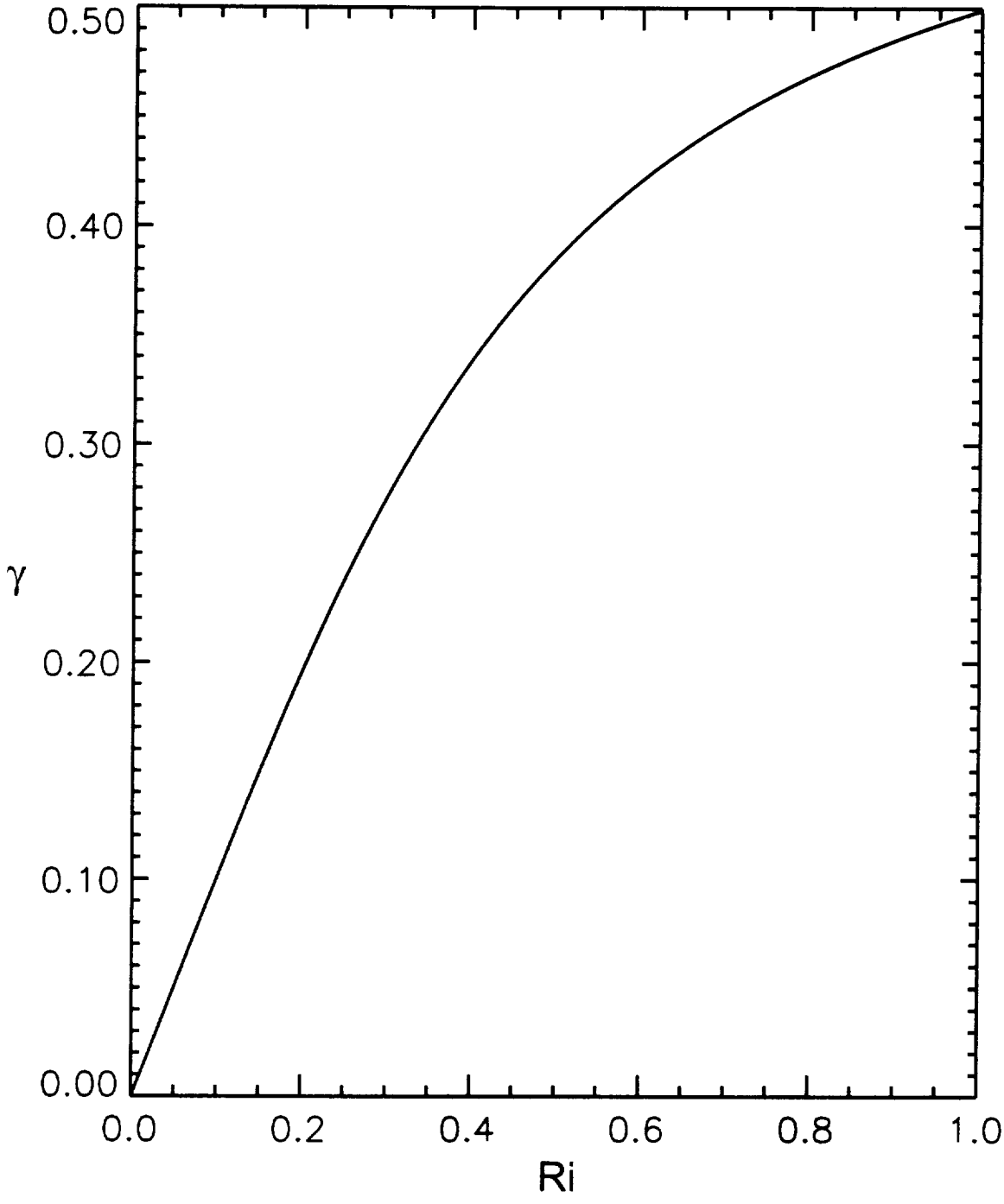

Fig. 7

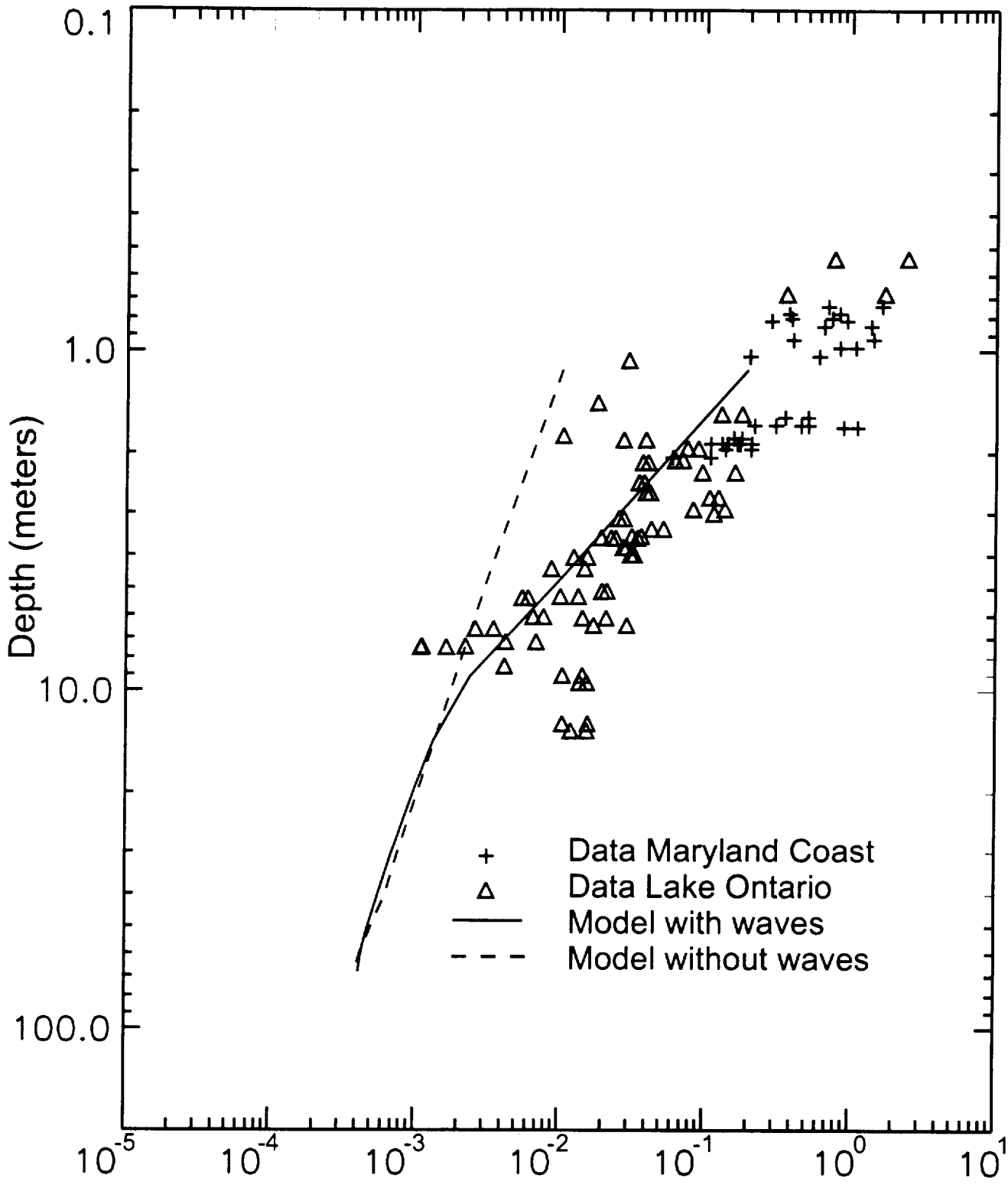
0.1
1.0
10.0
100.0
Depth (meters)
10^{-5}
10^{-4}
10^{-3}
10^{-2}
10^{-1}
10^{0}
10^{1}
Data Maryland Coast
Data Lake Ontario
Model with waves
Model without waves

Fig. 8

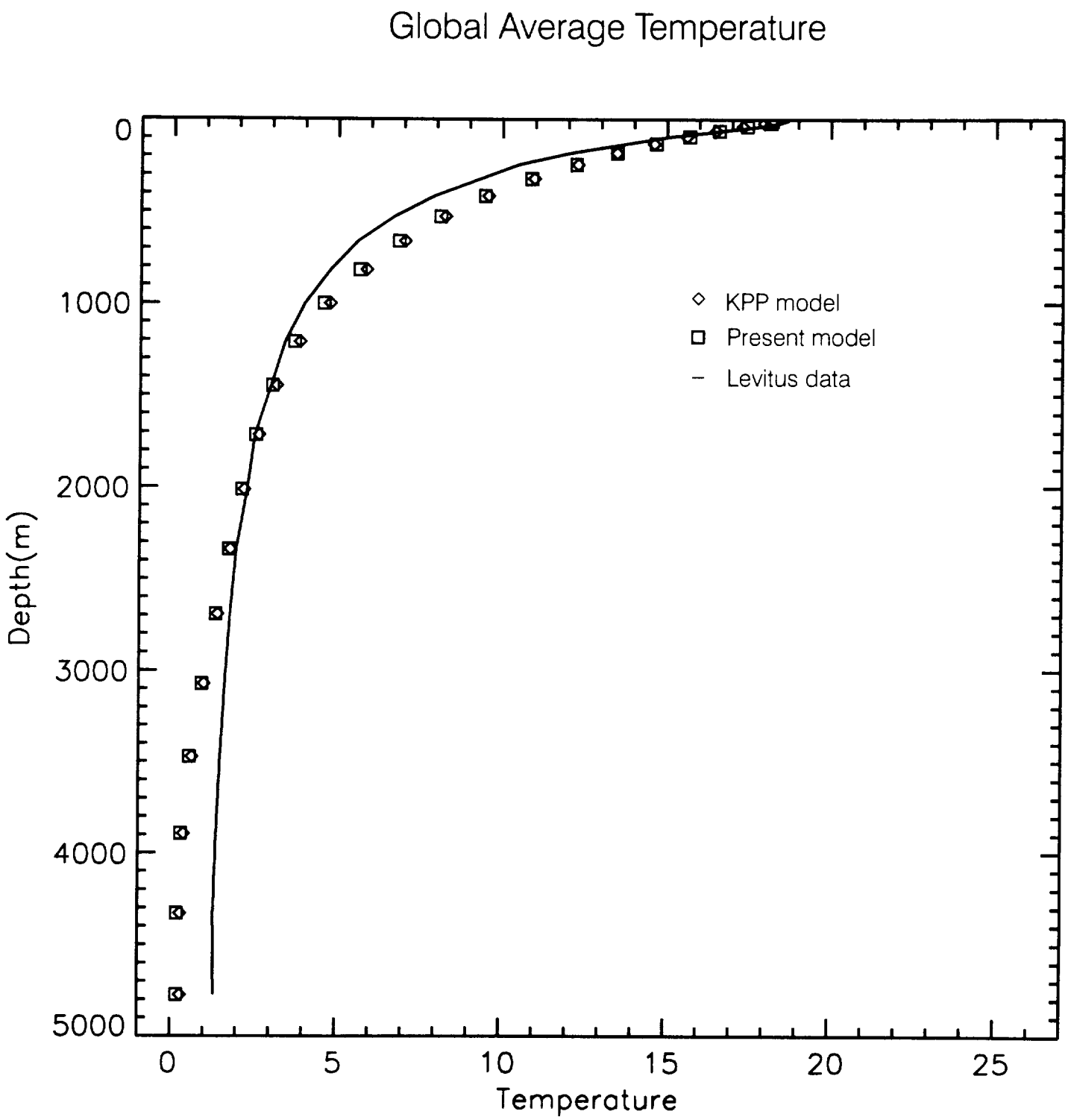
Global Average Temperature
0
1000
2000
3000
4000
5000
Depth(m)
0
5
10
15
20
25
Temperature
KPP model
Present model
Levitus data

Fig. 9

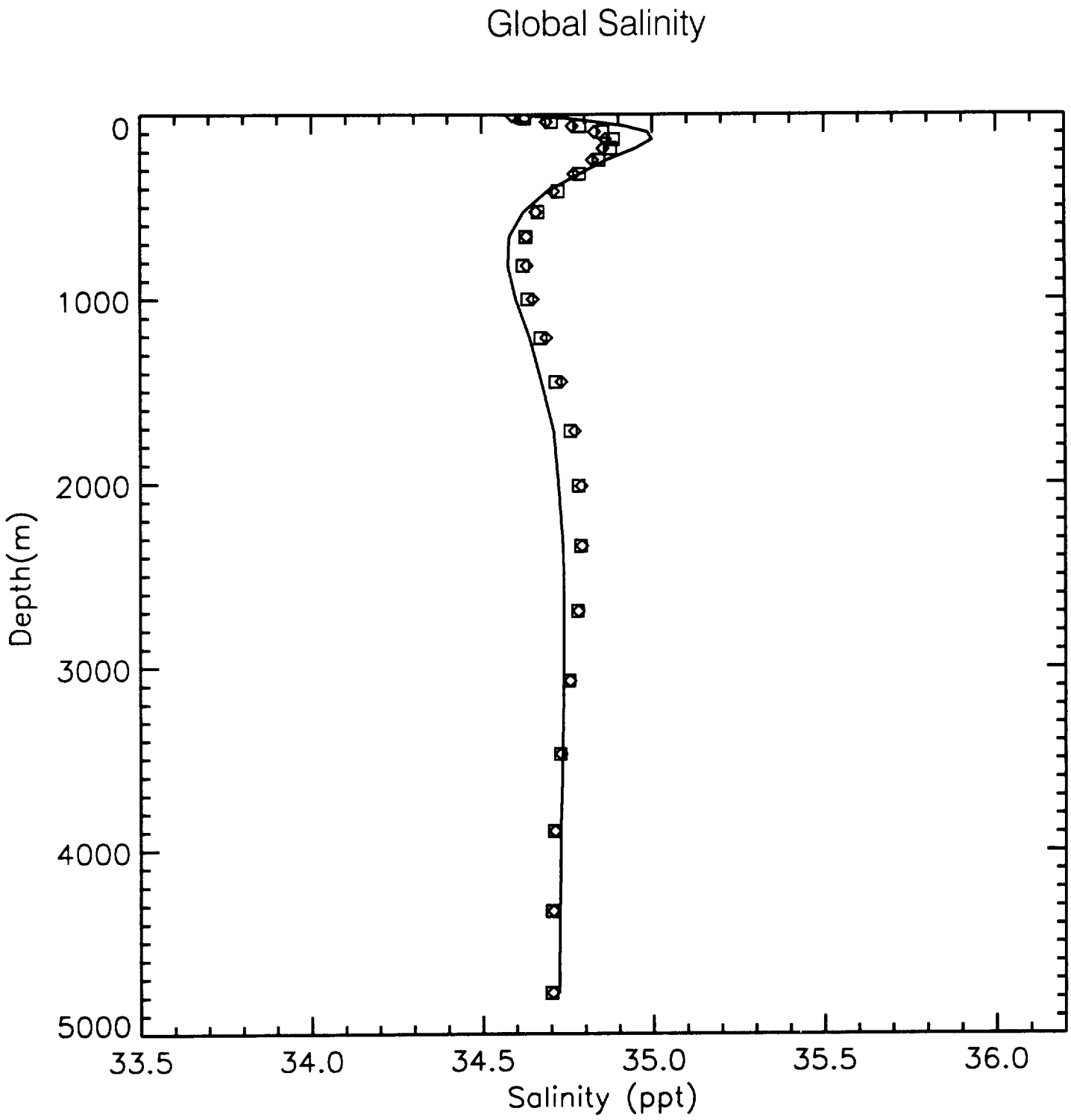
Global Salinity
0
1000
2000
3000
4000
5000
Depth(m)
33.5
34.0
34.5
35.0
35.5
36.0
Salinity (ppt)

Fig. 10

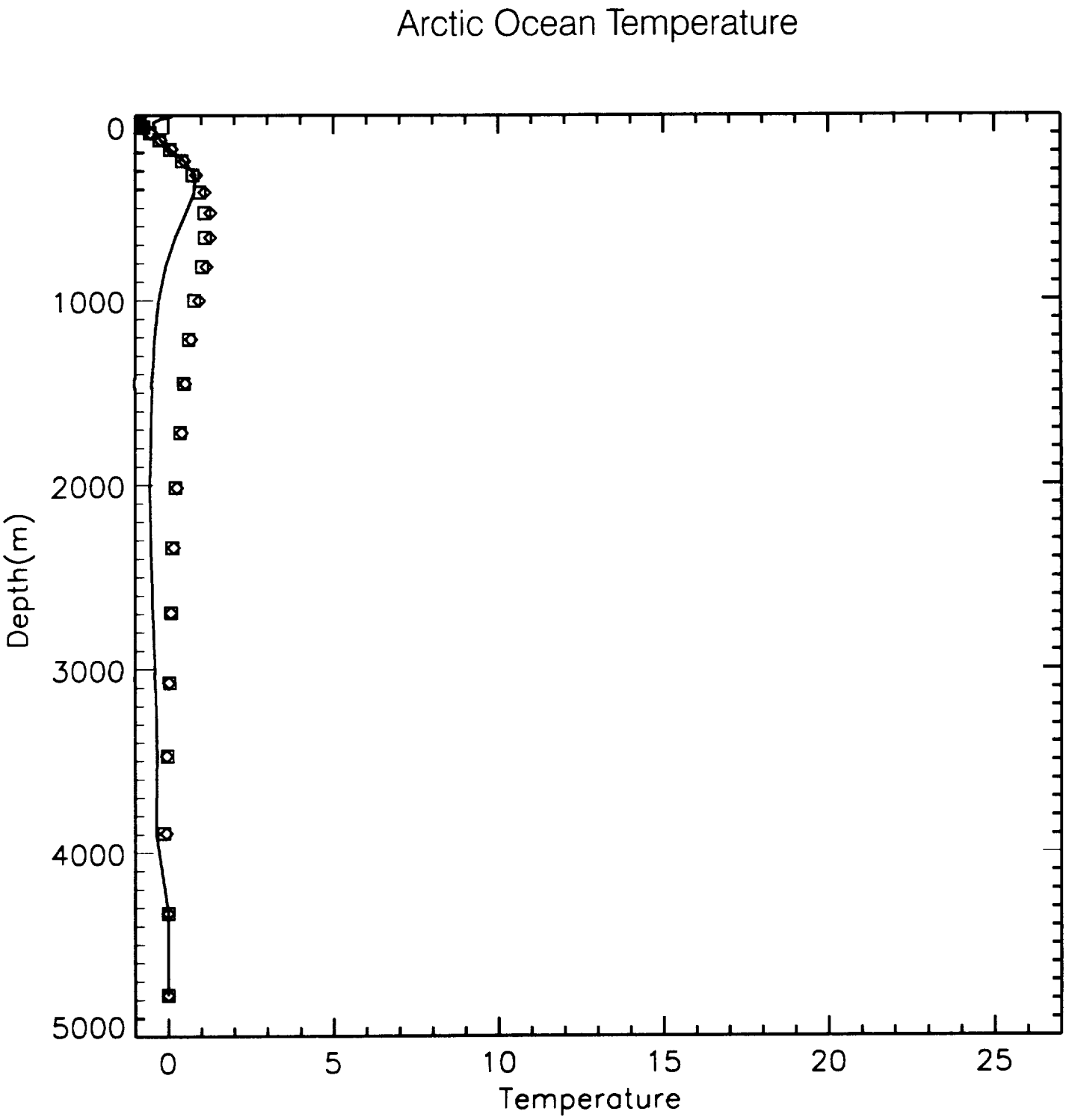
Arctic Ocean Temperature
0
1000
2000
3000
4000
5000
Depth(m)
0
5
10
15
20
25
Temperature

Fig. 11

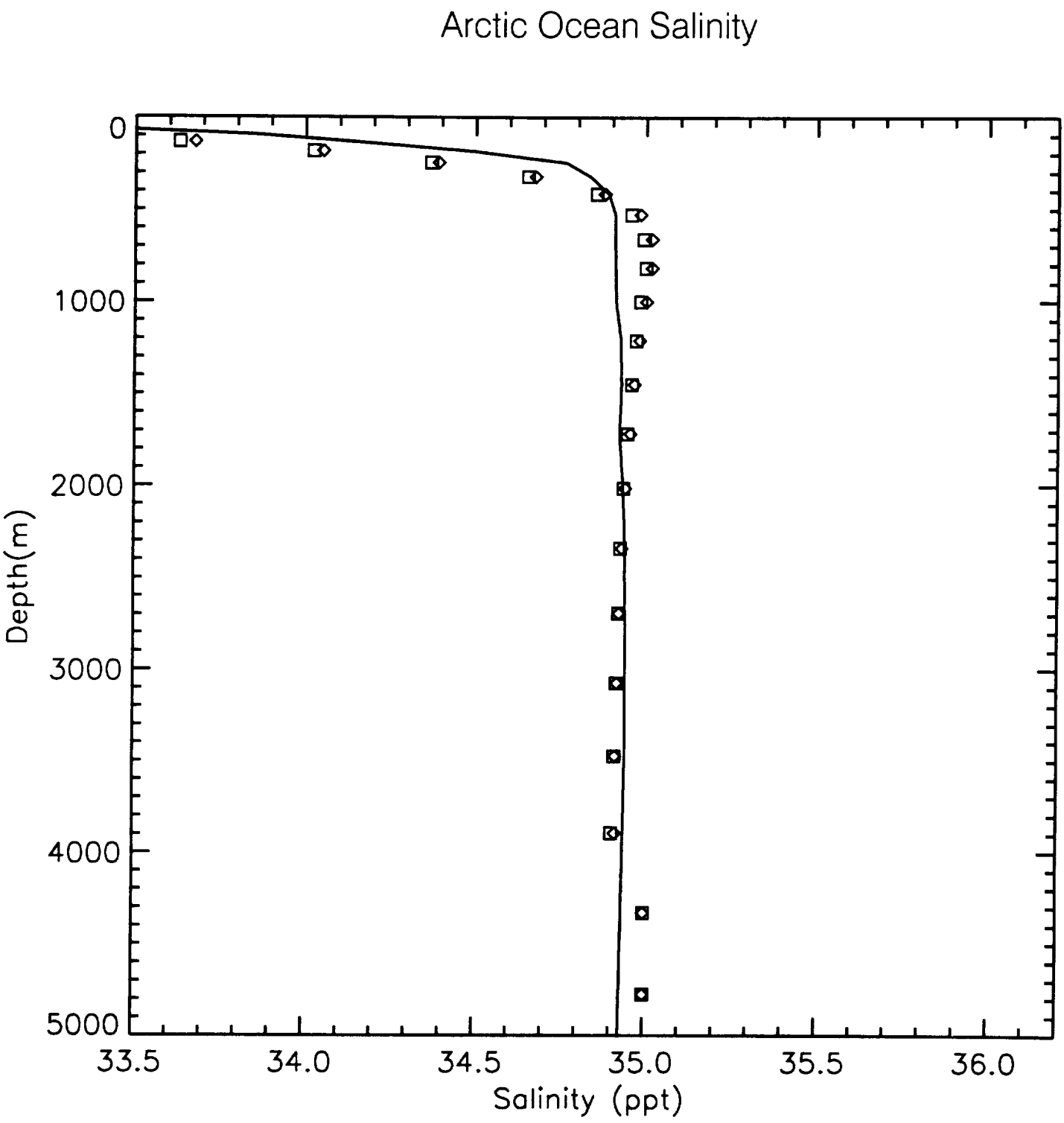
Arctic Ocean Salinity
0
1000
2000
3000
4000
5000
Depth(m)
33.5
34.0
34.5
35.0
35.5
36.0
Salinity (ppt)

Fig. 12

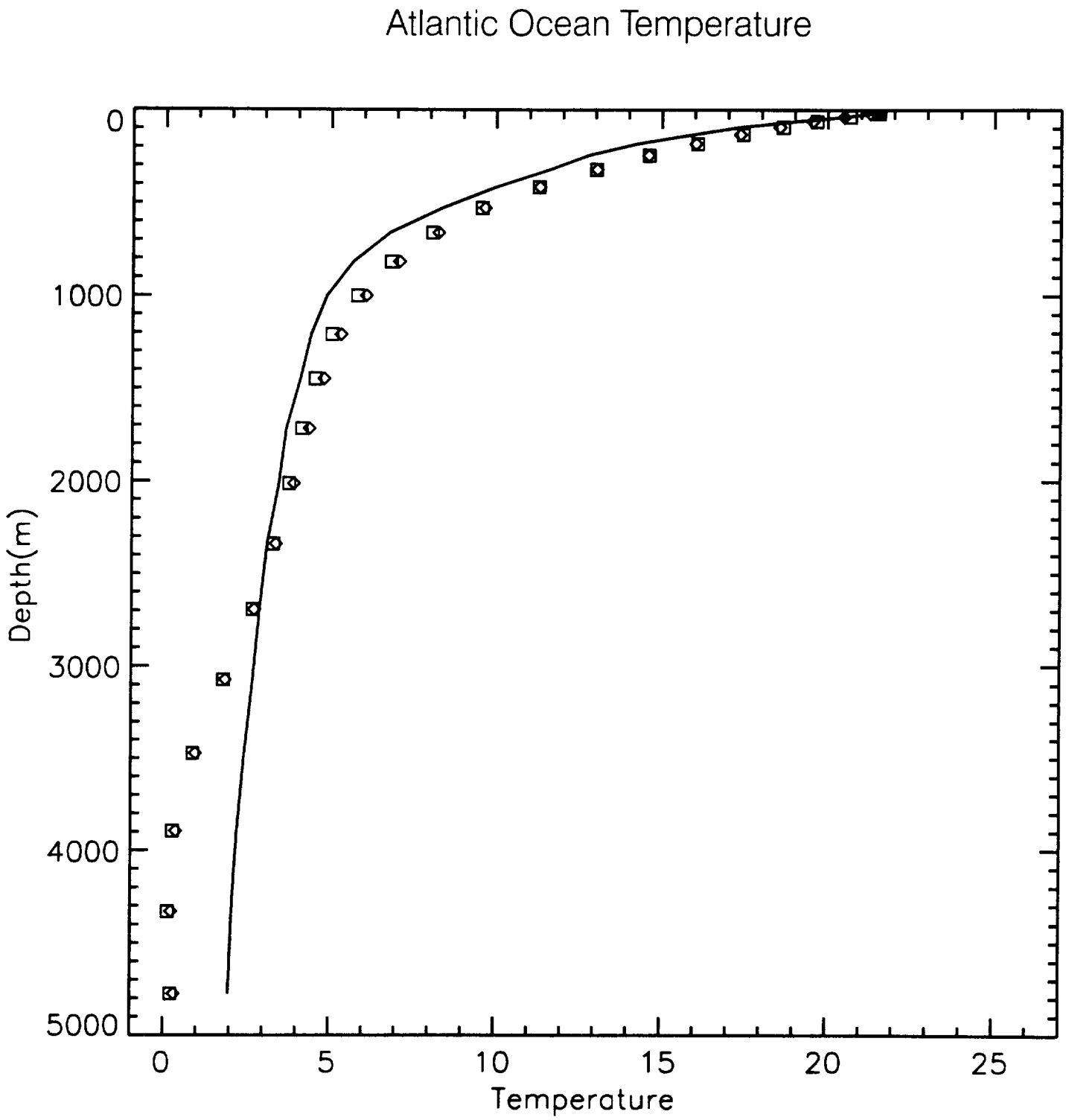
Atlantic Ocean Temperature
0
1000
2000
3000
4000
5000
Depth(m)
0
5
10
15
20
25
Temperature

Fig. 13

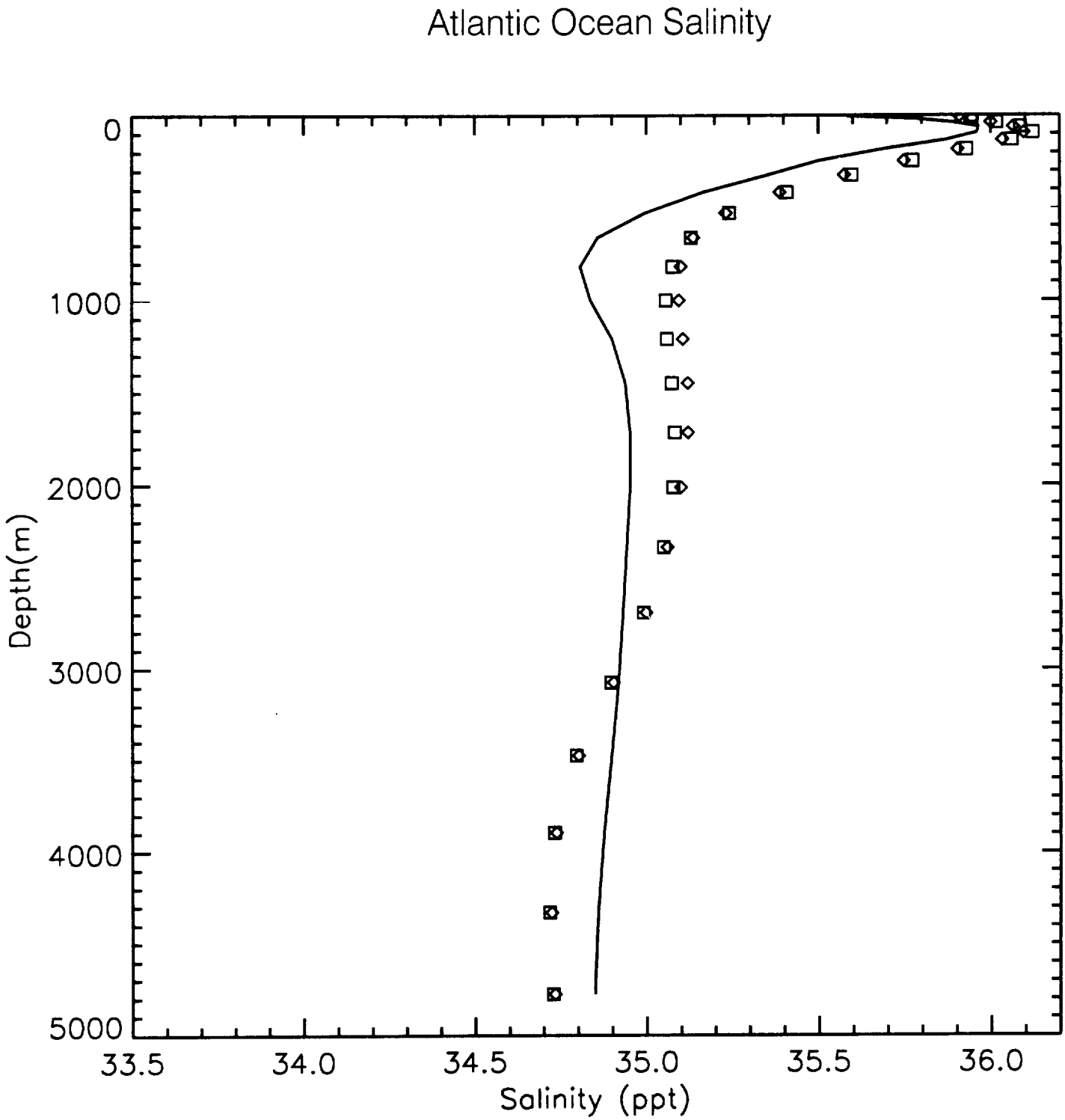
Atlantic Ocean Salinity
0
1000
2000
3000
4000
5000
Depth(m)
33.5
34.0
34.5
35.0
35.5
36.0
Salinity (ppt)

Fig. 14

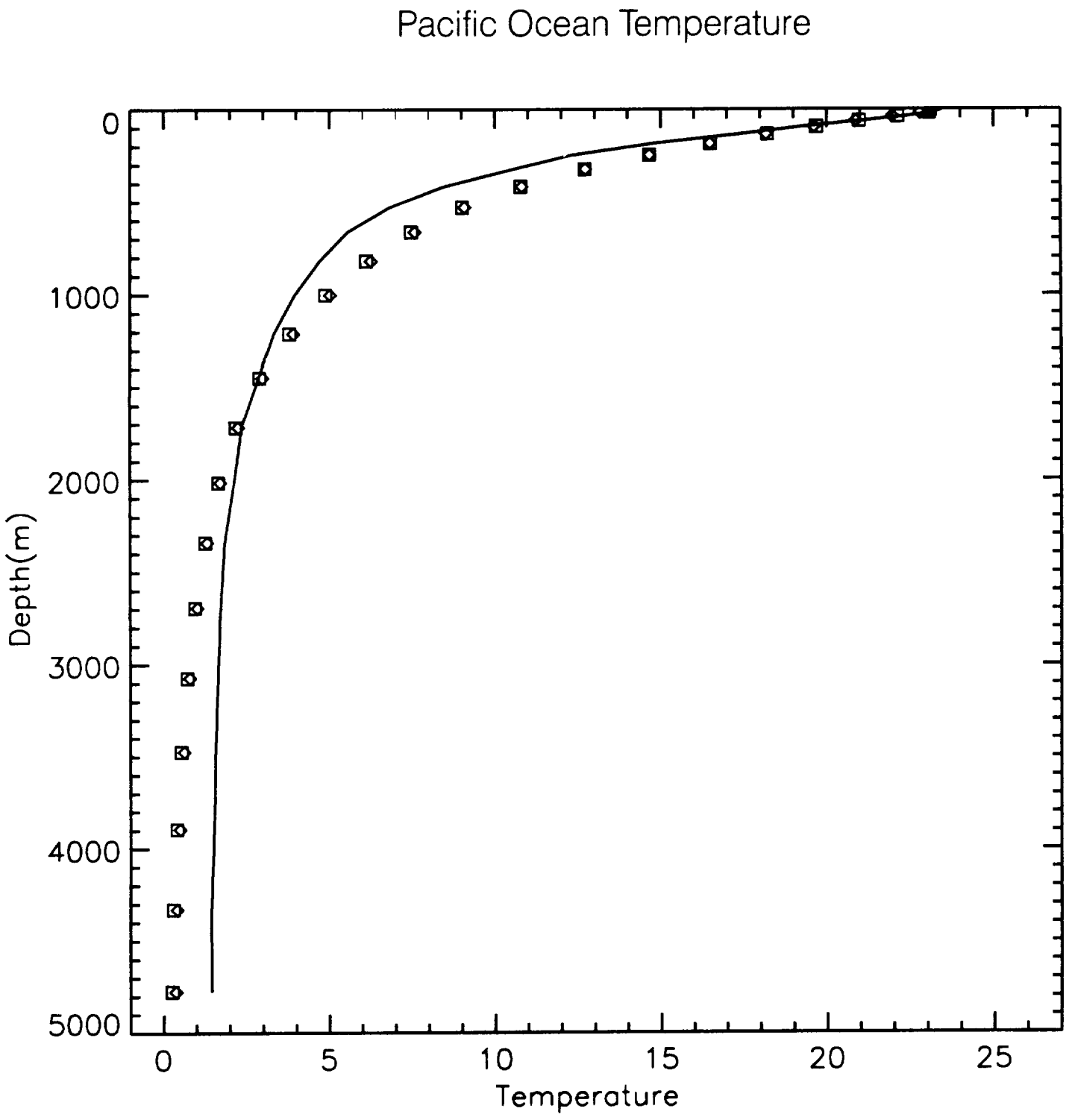
Pacific Ocean Temperature
0
1000
2000
3000
4000
5000
Depth(m)
0
5
10
15
20
25
Temperature

Fig. 15

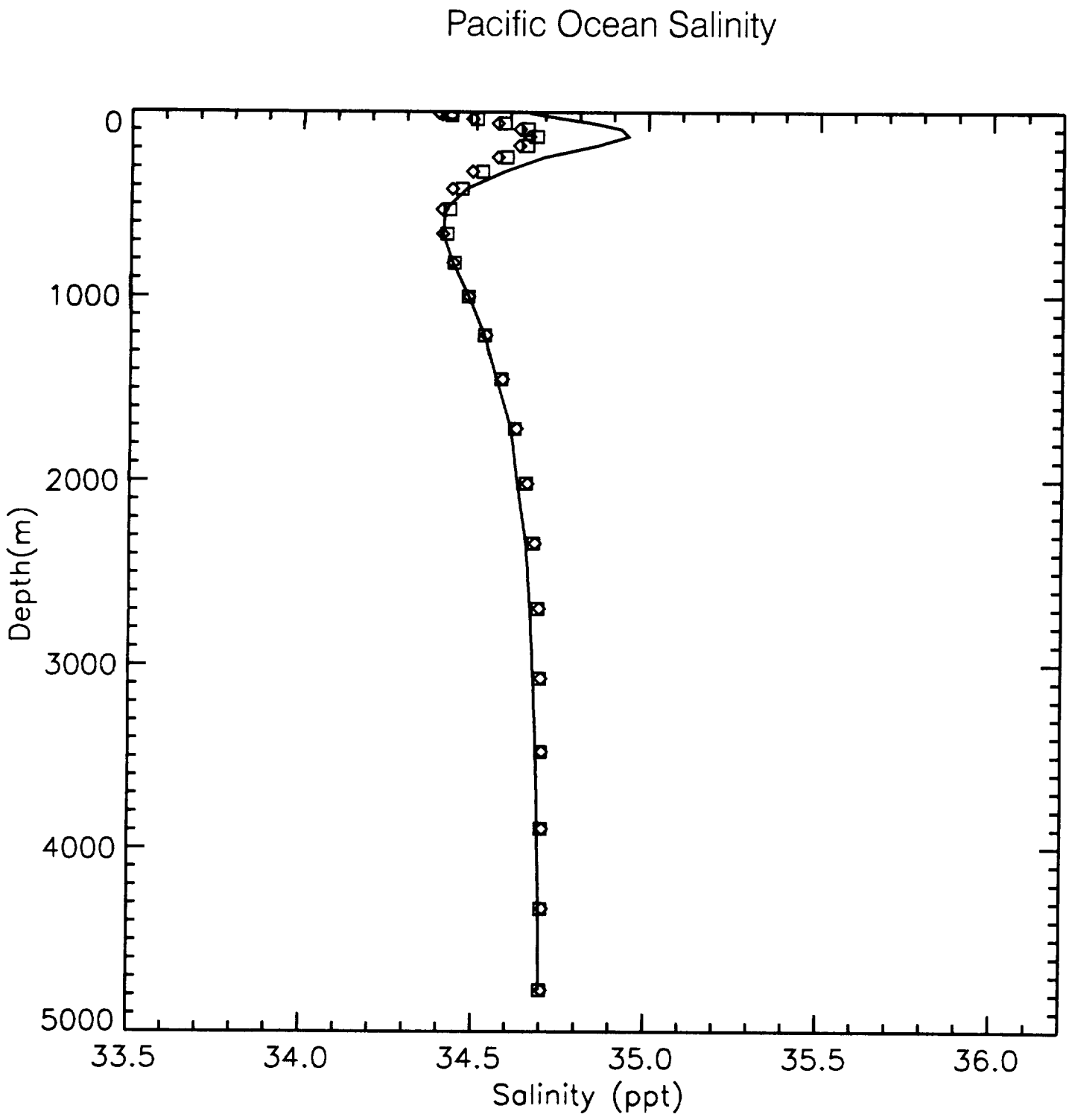
Pacific Ocean Salinity
0
1000
2000
3000
4000
5000
Depth(m)
33.5
34.0
34.5
35.0
35.5
36.0
Salinity (ppt)

Fig. 16

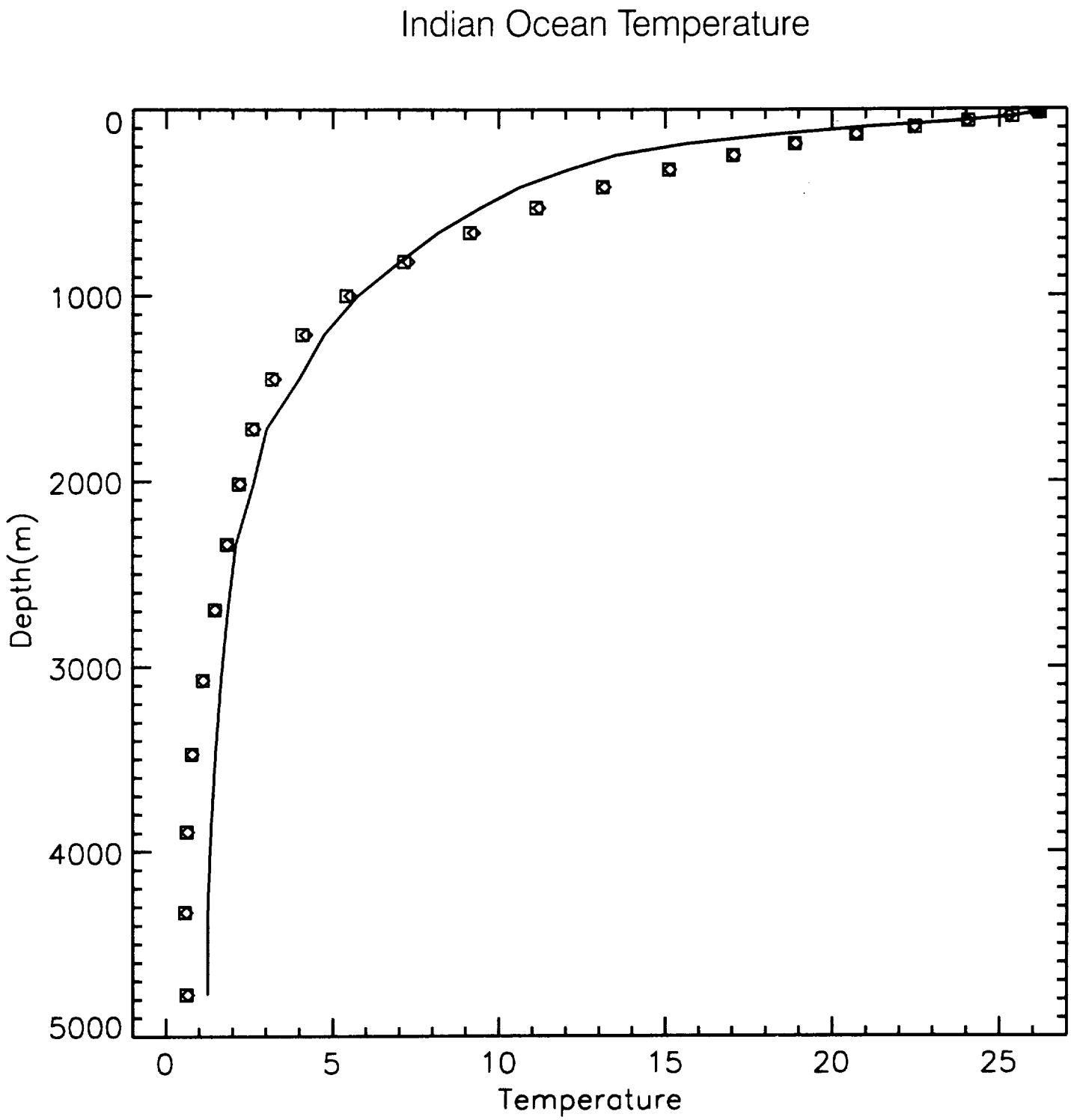
Indian Ocean Temperature
0
1000
2000
3000
4000
5000
Depth(m)
0
5
10
15
20
25
Temperature

Fig. 17

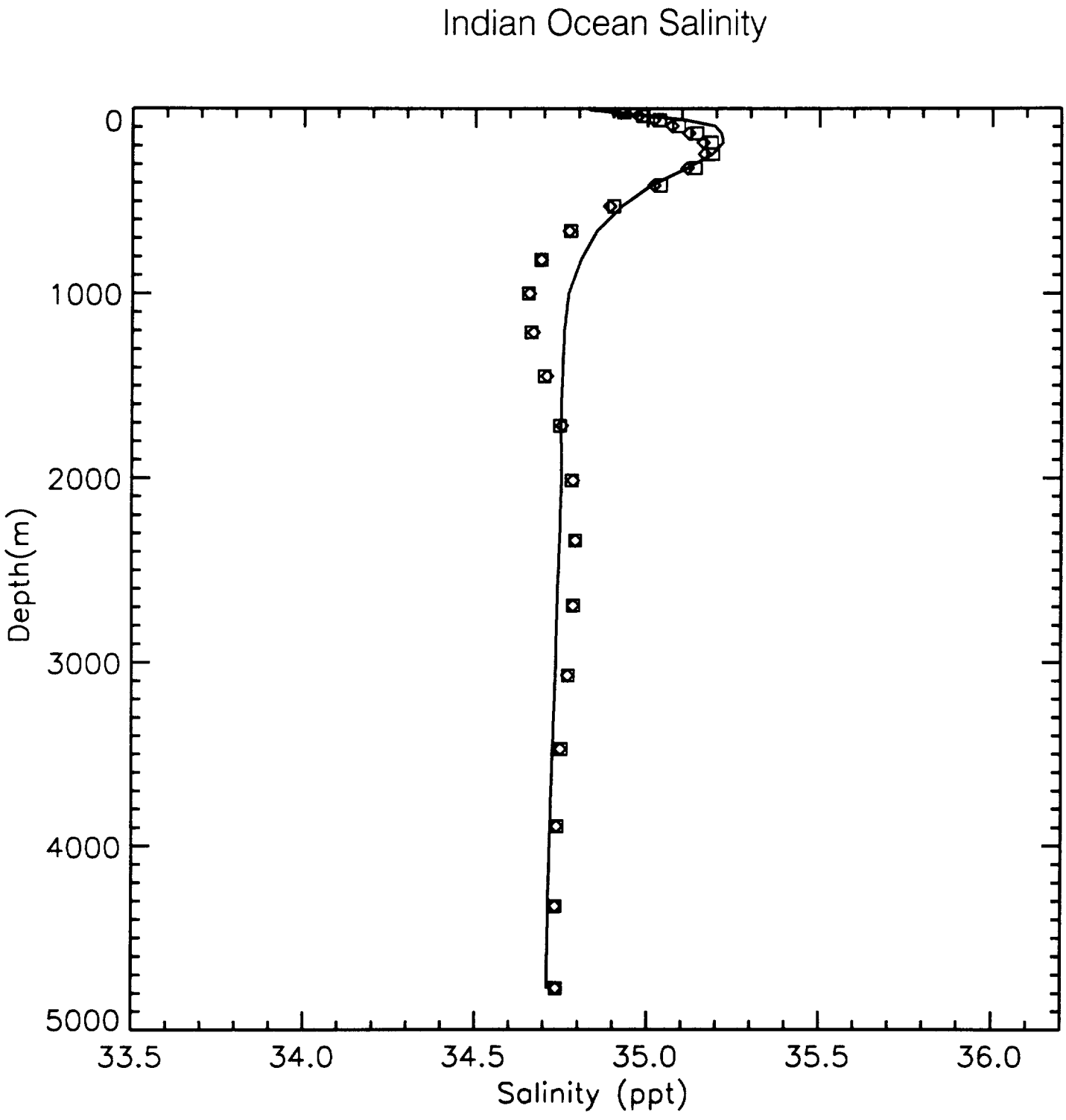
Indian Ocean Salinity
0
1000
2000
3000
4000
5000
Depth(m)
33.5
34.0
34.5
35.0
35.5
36.0
Salinity (ppt)

Fig. 18

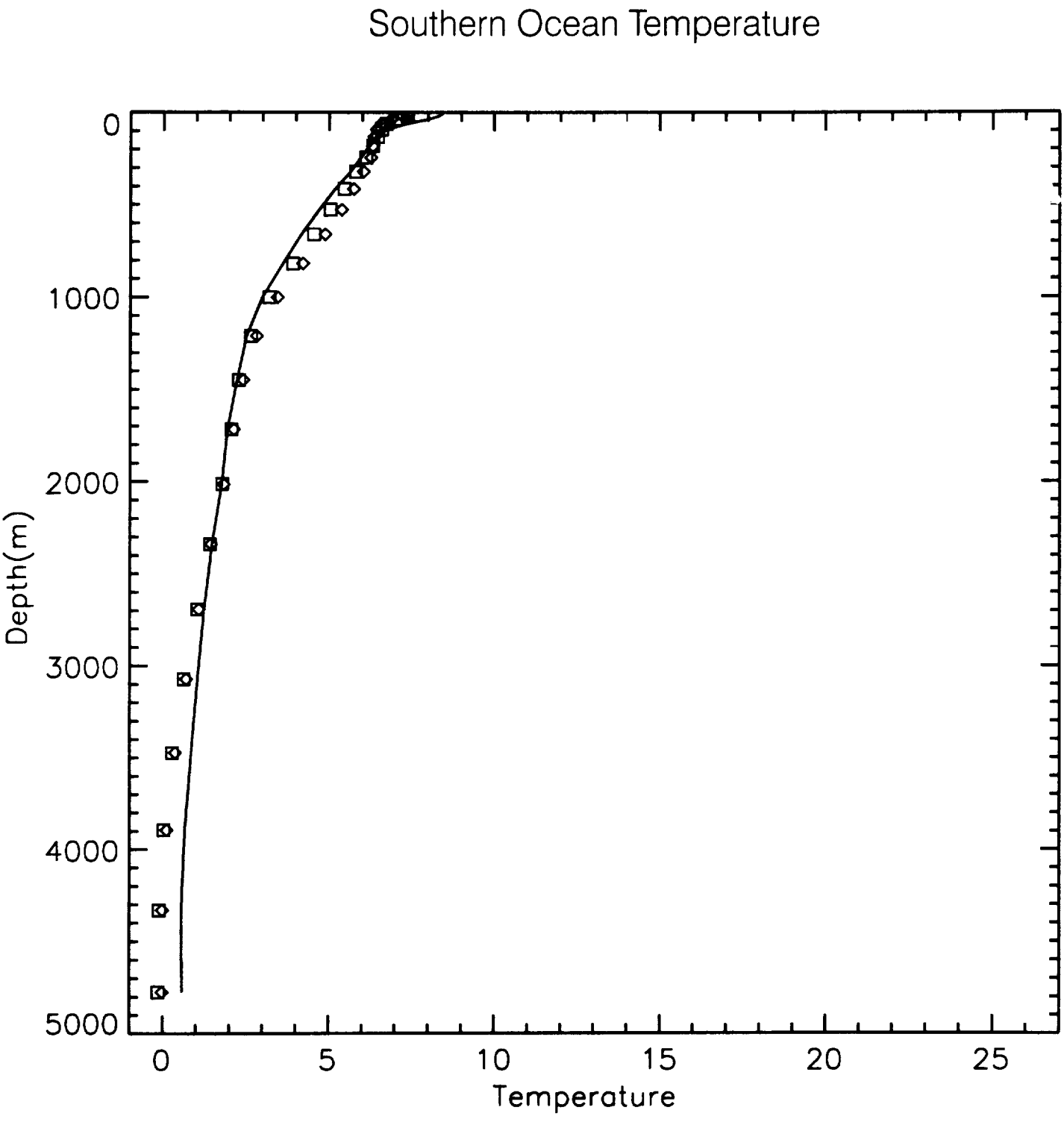
Southern Ocean Temperature
0
1000
2000
3000
4000
5000
Depth(m)
0
5
10
15
20
25
Temperature

Fig. 19

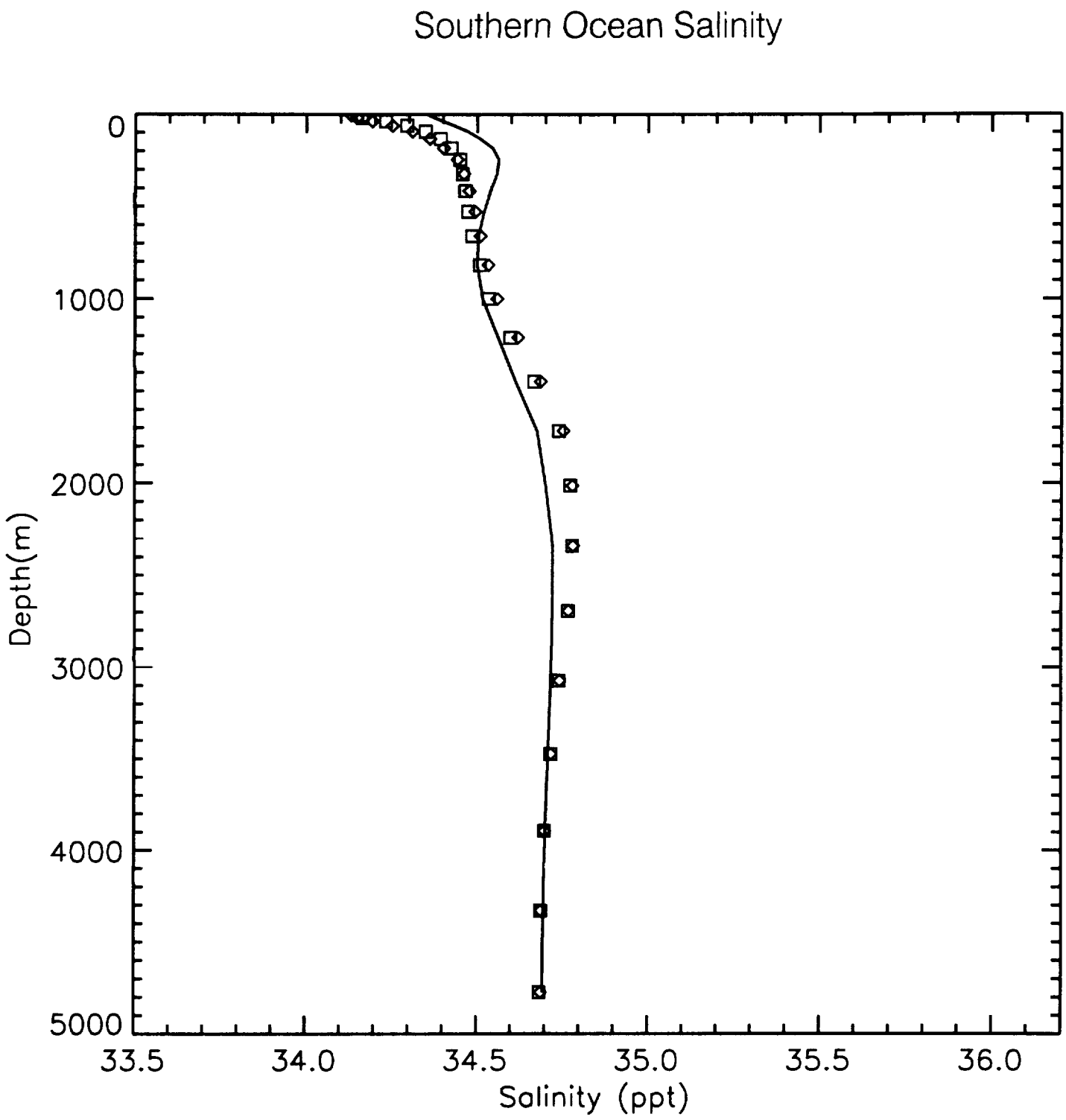
Southern Ocean Salinity
0
1000
2000
3000
4000
5000
Depth(m)
33.5
34.0
34.5
35.0
35.5
36.0
Salinity (ppt)

Fig. 20